HHS Public Access

Author manuscript

Exp Suppl. Author manuscript; available in PMC 2023 March 24.

Published in final edited form as:

Exp Suppl. 2022 ; 114: 179–213. doi:10.1007/978-3-030-93306-7_8.

The Function and Structure of the Microsporidia Polar Tube

Bing Han,

Department of Pathogenic Biology, School of Basic Medical Sciences, Cheeloo College of Medicine, Shandong University, Jinan, China; Department of Pathology, Albert Einstein College of Medicine, New York, USA

Peter M. Takvorian,

Department of Pathology, Albert Einstein College of Medicine, New York, USA; Department of Biological Sciences, Rutgers University, Newark, NJ, USA

Louis M. Weiss

Department of Pathology, Albert Einstein College of Medicine, New York, USA; Department of Medicine, Albert Einstein College of Medicine, New York, USA

Abstract

Microsporidia are obligate intracellular pathogens that were initially identified about 160 years ago. Current phylogenetic analysis suggests that they are grouped with Cryptomycota as a basal branch or sister group to the fungi. Microsporidia are found worldwide and can infect a wide range of animals from invertebrates to vertebrates, including humans. They are responsible for a variety of diseases once thought to be restricted to immunocompromised patients but also occur in immunocompetent individuals. The small oval spore containing a coiled polar filament, which is part of the extrusion and invasion apparatus that transfers the infective sporoplasm to a new host, is a defining characteristic of all microsporidia. When the spore becomes activated, the polar filament uncoils and undergoes a rapid transition into a hollow tube that will transport the sporoplasm into a new cell. The polar tube has the ability to increase its diameter from approximately 100 nm to over 600 nm to accommodate the passage of an intact sporoplasm and penetrate the plasmalemma of the new host cell. During this process, various polar tube proteins appear to be involved in polar tube attachment to host cell and can interact with host proteins. These various interactions act to promote host cell infection.

Keywords

Microsporidia; Spore; Polar filament; Polar tube proteins; Spore wall proteins; Cell-host interaction; Diagnosis; Microsporidiosis

* louis.weiss@einsteinmed.edu .

Conflict of Interest The authors declare that there is no conflict of interest.

Compliance with Ethical Standards

Ethical Approval All applicable international, national, and/or institutional guidelines for the care and use of animals were followed.

8.1 Introduction

Microsporidia are a diverse group of spore-forming, unicellular obligate intracellular parasites (Fig. 8.1a). The identification of the first recognized microsporidia *Nosema bombycis* was in 1857; since that initial description, over 200 genera and 1700 species of microsporidia have been identified over the past 160 years. Phylogenetic analysis suggests that microsporidia are related to fungi, being grouped with Cryptomycota as a basal branch or sister group to fungi (James et al. 2013). The genome size of the microsporidia varies from 2.18 to 51.35 Mb coding for 2000–5000 proteins. The genomic size of Encephalitozoonidae is less than 2.5 Mb, making them among the smallest eukaryotic genomes described to date (Weiss and Vossbrinck 1999; Katinka et al. 2001). Genome data for the microsporidia are available online at MicrosporidiaDB.org (https://microsporidiadb.org/micro/), which is part of the VEuPath database (https://veupathdb.org/veupathdb/) (Aurrecoechea et al. 2011).

Microsporidia can cause localized or disseminated infection in humans (Sak et al. 2011; Didier and Weiss 2011), and currently there are 17 species of microsporidia, in 10 genera, that have been reported to infect humans (Visvesvara 2002; Juarez et al. 2005). These human-infecting microsporidia are responsible for a variety of diseases, and while infections were initially thought to be restricted to immune-compromised patients, it is now known that infection can also occur in immune-competent individuals (Ramanan and Pritt 2014; Weiss 2020). The clinical manifestations of microsporidiosis are diverse, varying depending on the causal species, the host immune status, and the mode of transmission. Disease manifestations include diarrhea, keratoconjunctivitis, cholangitis, kidney and urogenital infection, myositis, ascites, hepatitis, sinusitis, disseminated infection, and asymptomatic infection (Weiss 2014, 2020; Weber et al. 2000; Desportes-Livage and Datry 2005).

Microsporidia can infect a wide range of hosts, including humans, and the manner of transmission and source of human infection vary depending on the species. Foodborne and waterborne transmission occurs (Stentiford et al. 2016a; Orlandi et al. 2002). Microsporidia spores have been identified in urine, feces, and infected animal carcasses, and these spores can eventually enter into water sources, which will contaminate recreational and potable water (Paterson and Lima 2015; Moss and Snyder 2017). Some species of microsporidia can infect both human and animals, indicating that zoonotic transmission is possible. For example, studies on urban pigeons infected by *Encephalitozoon intestinalis* and *Encephalitozoon hellem* revealed that there is no barrier to microsporidia transmission between park pigeons and humans (Haro et al. 2005).

The environmentally resistant microsporidian spore contains a unique structure, the invasion apparatus that contains a single-coiled polar tube (within the spore, the polar tube is often referred to as the polar filament) (Han et al. 2020). The spore is the terminal and infectious stage of the microsporidial life cycle and the only viable stage that can survive outside of the host cell which enables it to endure harsh extracellular environmental conditions (Yang et al. 2018). Spore wall proteins are probably involved in the processes of spore adherence, signaling, and other interactions with host cells (Southern et al. 2007). The polar tube is a highly specialized structure involved in invasion of host cells (Xu and Weiss 2005). Polar

tubes are found in all microsporidial species. Generally, the polar tube (often called the polar filament when it is within the spore) tightly coils within the spore and forms a spring-like structure (Jaroenlak et al. 2020). Upon appropriate environmental stimulation, the polar tube will rapidly discharge out of the spore, and the tip of the polar tube will contact and interact with the host cell serving as a conduit for the nucleus and sporoplasm passage into the new host cell (Han et al. 2017). Due to the importance of the polar tube during invasion by microsporidia, the formation of the polar tube, the structure, its protein composition, and the mechanism of polar tube eversion have drawn the interest of scientists for the last six decades (Han et al. 2020).

8.2 Structure of the Microsporidian Spore and Germination

Although diverse, all microsporidia produce a specialized, resistant, extracellular stage, the spore, which encloses and protects the infective sporoplasm and the invasion apparatus. Spores are generally small, oval- or pyriform-shaped, and range in size from 1 μm to 12 μm (Vavra 1976). Those infecting mammals are generally 1–4 μm in length (Weber et al. 1994).

Several imaging techniques have been used to identify and study the microsporidian spore and polar tube extrusion. Differential interference contrast (DIC) and phase contrast (PC) microscopy both enable the observation of live unfixed, unstained spores. This is especially useful when studying spore activation, polar tube extrusion (Fig. 8.1b), and the transport of the infective sporoplasm (Fig. 8.1c). Scanning electron microscopy (SEM) has been very useful for obtaining three-dimensional images of the exterior surface of spores and their extruded polar tubes (Fig. 8.2a). Transmission electron microscopy (TEM) has been the imaging tool most frequently used to study spore structure and its contents, since Huger (Huger 1960) published the first TEM images of a microsporidian spore (Weiss and Bechnel 2014). This technique is particularly useful for imaging microsporidia, due to the small size of the microsporidian spore and its extensive membrane systems, infection apparatus (polar filament), and sporoplasm, all tightly packed inside the spore. When observed with TEM, microsporidian spores have an electron-dense outer spore coat overlying an inner thicker lucent coat followed by a membrane system surrounding the spore contents and polar filament coils. The spore contents include an anterior anchoring disk complex, tightly packed arrays of membrane clusters (the lamellar polaroplast and flattened tubules), and a centrally located sporoplasm, composed of scant cytoplasm containing a single nucleus or pair of abutted nuclei (diplokaryon), tightly packed ribosomes, some endoplasmic reticulum, and Golgi (Fig. 8.2b). Surrounding the central region of the spore is a coiled polar filament (termed the polar tube when extruded) (Cali and Takvorian 2014; Vavra 1976). The polar filament/polar tube when exiting the spore transports the sporoplasm through itself into a host cell. Inside of the spore, cross-sectional images of the polar filament indicate that it is a solid structure composed of alternating concentric rings of electron-dense and lucent material surrounding electron-dense material in the center (Fig. 8.2b) (Cali and Takvorian 2014; Vavra 1976). The number of coils and their contents varies in different organisms (Cali and Takvorian 2014; Vavra 1976).

Due to the density of the spore wall and extreme packing of its contents, traditional TEM studies using thin sections (60–90 nm) have not provided the images needed to

fully understand the organization of the spore contents. In an attempt to better understand the internal structures and their location, our laboratory group has utilized high-voltage transmission electron microscopy (HVTEM), taking multiple tilt angle images of 400-nm-thick sections of spores (Fig. 8.3a) and generating three-dimensional (3-D) computerized models (Fig. 8.3b and c). During activation and extrusion, the internal organization of the spore undergoes massive membrane reorganization with the “solid” polar filament becoming a hollow tube as it everts and exits the spore (Cali and Takvorian 2014; Vavra 1976; Chioralia et al. 1998; Cali et al. 2002). The long (50–500 μm) narrow (90–120 nm) polar tube transfers the relatively large (1–1.5 μm) infective sporoplasm from the spore into a host cell in less than 2 seconds (Frixione et al. 1992; Jaroenlak et al. 2020).

Recently, Jaroenlak et al. (2020) utilized serial block-face scanning electron microscopy (SBFSEM) imaging of intact *Anncaliia algerae* and *Encephalitozoon hellem* spores to study their three-dimensional organization. Utilizing fixed cells cut at 50 nm, the authors imaged the cells and then stacked the images and segmented areas of interest to produce 3-D models of the spore contents. Models generated of the spore and the intact polar filament indicated that the polar filament coils in a right-hand helix (Fig. 8.4a, b, c). The authors’ live cell studies determined the polar tube extrudes and reaches its full length under 1 second and that the sporoplasm which is about seven times larger than the polar tube diameter remains intact as it passes through the polar tube (see Chap. 9).

An additional method of imaging that has been utilized recently to examine the spore and its internal contents is focused ion beam scanning electron microscopy (FIB-SEM) which can utilize the same specimen blocks used for TEM (Fig. 8.5a). The ion beam can be used to cut/mill a cross-section of the sample to obtain information from regions of interest beneath the sample surface. A complete volume of a sample can be achieved by repeated milling of thin slices and imaging of the new surfaces. The captured images of the spores can be as thin as 10 nm. The captured images are aligned, stacked, and segmented to produce 3-D models similar to those obtained by HVTEM and SBFSEM with the use of computer programs such as Amira©. FIB-SEM software can produce tomograms from the approximately 200 images of a 2-μm-thick spore when cut at 10 nm and 150 images at 15 nm cuts. FIB-SEM images (15-nm spaced “Z” stack) of activated *Anncaliia algerae* spores demonstrate the polar tube in a coil with a straight portion of the tube exiting the spore through the thin anterior portion of the exospore (Fig. 8.5b). The extruding polar tube passes through the anchoring disc-polaroplast complex of an extended “collar” of at least three layers: the erupted exospore, the anchoring disc, and the polaroplast. The 3-D color model of the spore, PT, anchoring disc complex, and posterior vacuole and membranes provides a perspective of the organization of the active extruding spore contents (Fig. 8.6a). Removal of the exospore wall and rotation of the model to show the anterior aspect of the PT and anchoring disc complex provide a view of the exiting PT passing through the complex as it uncoils and straightens (Fig. 8.6b).

8.3 Polar Filament Development and Formation

The vast majority of microsporidia undergo a three-part developmental cycle which starts with entry of the sporoplasm into a host cell. The first part is proliferation to increase the

numbers of organisms, followed by sporogony, in which the “simple” proliferative cells undergo a complex morphological change into sporoblasts. These cells elongate and secrete electron-dense material on their surface which will become the exospore coat, and then synthesis of the polar filament components begins. The synthesis of the polar filament occurs in sporoblasts which contain a large Golgi (Beznoussenko et al. 2007; Takvorian and Cali 1994). The morphogenesis of the polar filament is first observed in early sporoblasts as an “oval body” of membranes and dense material (Takvorian and Cali 1996). The Golgi is involved in the formation of the polar filament, and polar filament proteins are assembled and posttranslationally modified by the Golgi. Enzyme histochemical reaction products generated by both the *cis*- and *trans*-Golgi (Takvorian and Cali 1994, 1996) surrounding the forming polar filament can be observed by TEM (Fig. 8.7a). During polar filament development, it is thought that polar tube proteins (PTP) are glycosylated. This is consistent with immunogold labeling of extruded polar tubes with concanavalin A (Con A), a lectin which binds to specific sites of glycosylation (Fig. 8.7b) (Xu et al. 2004; Takvorian and Cali 1996). Eventually the filament coils around the inner aspect of the endospore, encased by a labyrinth of membranes surrounding the outer sporoplasm-limiting membrane, indicating that the polar filament is probably external to the sporoplasm contents (Cali et al. 2002).

The diameter, length, and arrangement of polar filament coils in the spore are variable and dependent on the species of microsporidia. The number of coils present can vary depending on species from 4 to approximately 30 (Weiss et al. 2014). There are two regions of the polar filament: the anterior straight portion which connects to the anchoring disk in the anterior end of the spore and the medial-posterior coiled region (Huger 1960; Vavra 1976). The average diameter of the typical polar filament is 90–120 nm in the coiled region, and the straight portion often has a somewhat larger diameter (Chioralia et al. 1998; Takvorian and Cali 1986). Generally, the straight portion will extend to the middle part of the spore and then coils; however, in some species like *Spraguea americana* (formerly *Glugea americanus)*, the straight portion will extend all the way to the posterior part of the spore, then turn anteriorly, and start to coil (Chioralia et al. 1998; Takvorian and Cali 1986; Vavra 1976) (Vavra 1976; Chioralia et al. 1998; Takvorian and Cali 1986).

8.4 The Structure of the Polar Tube

Although it has been more than 60 years since Kramer in 1960 (Kramer 1960) demonstrated the passage of the infective sporoplasm from the spore through the polar tube and Huger’s (Huger 1960) first TEM images of the polar filament inside the spore, the polar tube structure, protein composition, extrusion mechanism(s), and sporoplasm transport are still enigmatic. The diameter of the extruded polar tube can increase from 100 to 600 nm during the passage of cargo and the sporoplasm, which illustrates the flexibility of the polar tube structural design (Weidner 1972; Lom and Vavra 1963; Weidner 1976). Cryo-transmission electron microscopy (CTEM) has been used to image vitreous frozen unfixed polar tubes and construct computer generated 3-D models of the structure of extruded polar tubes (Takvorian et al. 2020). This study demonstrated that the polar tube surface is covered with fine fibrillary material (Fig. 8.8a) which are probably the sites of modified glycoproteins on the surface of the polar tube (Fig. 8.7b). These polar tube CTEM images demonstrate various structures containing masses of tightly folded or stacked membranes, assorted cargo

(Fig. 8.8b), and that the polar tube has a closed tip that can form a terminal sac before the polar tube tip opens (Takvorian et al. 2020). Images of membrane clusters, cargo, and the sporoplasm traveling through the tube confirmed that the tube can expand its diameter to accommodate the items passing through it. An image of a greatly distended segment of the tube contained a sporoplasm shaped like a sperm head (Fig. 8.8c), which indicates that the sporoplasm traverses the polar tube as a fully intact membrane-bound cellular entity (Takvorian et al. 2020). Multiple aligned and stacked images (tomogram) of a portion of polar tube were segmented, and 3-D models were generated using Amira® software, enabling visualization of the cargo inside the tube and its surface structure. The polar tube surface was covered with tufts of fibrillar material, and its lumen contained membranes, cylinders, and assorted cargo (Fig. 8.9a, b, c, d).

8.5 Protein Composition of the Polar Tube

As noted previously, it was not until 1960 when Kramer demonstrated that the function of the microsporidian polar tube was to transport the infective sporoplasm out of the spore (Kramer 1960), and in the same year, Huger (1960) published the first TEM images of the spore (Huger 1960). These two reports sparked great interest in spore internal structure(s) and the composition and structure of the polar tube. Due to the spore's resilience and resistance to breakage and the difficulty of obtaining large quantities of purified spores, polar tube research was very slow for the next 30 years, despite the widespread interest in its development, structure, and function. Keohane et al. (Keohane et al. 1994; Keohane et al. 1996b) obtained massive quantities of *Spraguea americana* (formerly *Glugea americanus*) spores from centimeter-sized cysts of the optic chiasma and spinal nerves of infected American angler fish *Lophius americanus.* The microsporidian spores were purified, mechanically disrupted with glass beads in a bead beater®, and washed in 1% SDS and 9 m urea, leaving only empty spore shells and polar tubes (Fig. 8.10a). A similar approach was used to produce a polar tube preparation from spores of various Encephalitozoonidae purified from tissue cultures (Keohane and Weiss 1999; Keohane et al. 1999; Delbac et al. 1998a; Delbac et al. 2001). Due to the unusual solubility properties of the polar tube which resist dissociation in 1% SDS and 9 M urea but dissociate in various concentrations of 2-mercaptoethanol (2-ME) or dithiothreitol (DTT), polar tube protein 1 (PTP1) was isolated from ruptured microsporidian spores by treating them with DTT to solubilize the polar tube proteins (PTPs) followed by further purification of the PTPs by reverse-phase high-performance liquid chromatography (HPLC) (Keohane et al. 1994; Keohane et al. 1996b). Subsequently, antibodies were produced to various PTPs and employed for immune localization of these various PTPs utilizing immunofluorescence micros-copy (IFA) and/or immunogold electron microscopy (Immuno-EM) (Fig. 8.10b).

Studies of polar tube protein composition to date have identified six distinct PTPs (i.e., PTP1 to PTP6) that are found in most microsporidia (Table 8.1). The first PTP to be identified was PTP1 (Keohane et al. 1996a, c). Amino acid analysis of PTP1 from various microsporidia confirmed that PTP1 is a proline-rich protein containing significant amounts of O-linked mannosylation (Keohane and Weiss 1998; Xu et al. 2003; Xu et al. 2004). High proline content is a feature of several structural proteins including collagen and elastin. To this end, the proline content of PTP1 is consistent with the hypothesis that this protein should have

a high tensile strength and elasticity, as it is one of the main constituents of the polar tube and these properties would be important for discharge and passage of sporoplasm through the narrow polar tube (Keohane et al. 1996; Keohane et al. 1998; Delbac et al. 2001). Most microsporidian PTP1s have central amino acid repeat regions that are predominantly hydrophilic; however, these repeats differ in composition and number depending on the microsporidian species. The N- and C-terminus of the various microsporidian PTP1 display more conservation suggesting that these areas may have important structural or functional domains. An N terminal-signal sequence is cleaved to form the mature protein and is predicted to target PTP1 for processing through the endoplasmic reticulum and Golgi complex, which is consistent with morphologic observations of polar tube development.

Proteomic and immunologic approaches resulted in the subsequent identification of PTP2 and PTP3 (Delbac et al. 2001; Peuvel et al. 2002). PTP2 is found at the same genomic locus as PTP1. In general, PTP2 is more conserved among microsporidia than PTP1, and PTP2s in various microsporidia that have been identified are similar in molecular weight, basic isoelectric point (pI), high lysine content, and conservation of cysteine residues (Delbac et al. 2001). Some microsporidia (e.g., *Antonospora locusta*, *Anncaliia algerae*, *Paranosema grylli*, and *Tubulinosema ratisbonensis*) have more than one PTP2 gene; however, it is known that the functional significance of having multiple PTP2 protein isotypes is for the biology of these organisms (Polonais et al. 2013). PTP3 was found to be solubilized by SDS treatment of polar tubes, with no requirement for a reducing agent such as DTT, indicating that cysteine bonding is not critical for this protein (Peuvel et al. 2002). It has been suggested that PTP3 might be a scaffold protein that plays an important role during the formation of polar tube by interaction with other PTPs (Peuvel et al. 2002; Bouzahzah et al. 2010). PTP1, PTP2, and PTP3 can be purified as a complex using cross-linking agents suggested that they probably interact directly with each other in the polar tube (Peuvel et al. 2002; Bouzahzah et al. 2010). Further study using yeast two-hybrid methods demonstrated that PTP1 could interact with PTP1, PTP2, and PTP3 at both its C- and N-terminal subdomains, but not its central region (Bouzahzah et al. 2010). This is consistent with the hypothesis that the PTP1 central region, which is highly variable between microsporidia species, is not involved in protein-protein interactions that are needed to form the polar tube.

PTP4 was found by proteomic analysis of purified polar tubes coupled with IFA validation of identified proteins (Han et al. 2017; Weiss et al. 2014; Han and Weiss 2017). A unique epitope of *Encephalitozoon hellem* PTP4 was found to specifically localize to the tip of the polar tube and was shown to bind to the host transferrin receptor 1 (TfR1), which is one of the key receptor proteins in the clathrin-mediated endocytosis pathway (Han and Weiss 2017). An antibody to *Antonospora locustae* PTP4 demonstrates a similar localization to the tip of the polar tube (Weiss et al. 2014). The genes for PTP4 and PTP5 are usually clustered together in microsporidian genomes (e.g., *Anncaliia algerae*, *Encephalitozoon hellem*, *Encephalitozoon intestinalis*, and *Encephalitozoon cuniculi*) which is similar to what is observed with *ptp1* and *ptp2*, suggesting that *ptp4* and *ptp5* may have been linked in either evolution or expression (Weiss et al. 2014; Han and Weiss 2017). An antibody to recombinant PTP5 localizes to the polar tube (Weiss et al. 2014). Recently, a novel polar tube protein (PTP6) was identified from *Nosema bombycis*, a pathogen of silkworms. NbPTP6 was rich in histidine and serine and has multiple glycosylation sites. Further study

revealed that this new polar tube protein is capable of binding to the host cell surface indicating a potential role for PTP6 in the process of polar tube interaction with its host cell (Lv et al. 2020). PTP6 homologs can be found in the genomes of other microsporidia (Table 8.1).

In *Nosema bombycis*, several spore wall proteins (NbSWPs) that have been identified have demonstrated interactions with NbPTPs (Wu et al. 2008, 2009; Wang et al. 2007; Li et al. 2012; Dolgikh et al. 2005; Cai et al. 2011). Using IFA, several of these NbSWPs have been shown to localize to the proximal region of the polar tube in *Nosema bombycis* (Wu et al. 2008, 2009; Wang et al. 2007; Li et al. 2012; Dolgikh et al. 2005; Cai et al. 2011). However, homologs of these proteins have either not been demonstrated in the Encephalitozoonidae, or IFA staining with antibody to potential homologs has not shown similar polar tube localization in the Encephalitozoonidae.

8.6 Glycosylation of Polar Tube Proteins

Microsporidia Golgi are networks of highly anastomosing, and often varicose, tubules and are connected or associated with either the ER or the plasma membrane where the polar tube proteins are synthesized (Fig. 8.7a) (Xu et al. 2004; Takvorian and Cali 1996; Beznoussenko et al. 2007). Glycosylation of transported proteins is one of the main functions of the Golgi. Despite microsporidia lacking the genes encoding the *N*-linked glycosylation machinery as well as the “classical mammalian” *O*-linked glycosylation genes, α-1, 2-mannosyltransferase, which is considered to be Golgi-specific, has been found in microsporidian genomes (Katinka et al. 2001; Lussier et al. 1997). Thus, during sporogony, when microsporidia transport PTPs via the Golgi, various PTPs could be mannosylated by the Golgi-specific-α-1, 2-mannosyltransferase resulting in posttranslational glycosylation of several PTPs (Fig. 8.7b) (Beznoussenko et al. 2007; Han et al. 2017; Lv et al. 2020).

PTP1 is a major polar tube component which accounts for at least 70% of the mass of the polar tube (Keohane et al. 1998). Sequence prediction based on the primary amino acid sequence of PTP1 demonstrates several potential *N*-and *O*-linked glycosylation sites (Xu et al. 2003). Analysis of EhPTP1 by mass spectrometry demonstrated it was larger than predicted by its primary amino acid sequence, and HPLC purification of native PTP1 demonstrated a sawtooth pattern when the peak is spread out with a shallow acetonitrile graduation, suggesting the presence of posttranslational modifications on PTP1 (Xu et al. 2004). A lectin overlay assay demonstrated that ConA reacts with α-mannose residues bound to PTP1 (Xu et al. 2004). In addition, PTP1 could be purified from a DTT-solubilized polar tube mixture by ConA affinity chromatography (Xu et al. 2004). These data indicate that PTP1 contains O-linked mannosylation residues to which ConA binds (Xu et al. 2004). These posttranslational modifications were further confirmed by an immunoprecipitation assay using radiolabeled mannose and glucosamine in *Encephalitozoon cuniculi* (Bouzahzah and Weiss 2010). O-mannosylation of PTP1 might be crucial for the invasion process by protecting the polar tube from degradation in the gastrointestinal tract of hosts. In many eukaryotic pathogens, protein glycan modifications are involved in host pathogen interactions and contribute to adherence and invasion (Varki 1993). Binding of PTP1 with ConA suggested that PTP1 may interact with host cell membrane mannose-binding

molecules such as dectin-2, mannose-binding lectin-MBL, and C-type lectin receptors during microsporidian infection and facilitate infectivity and adherence of the polar tube to the host cell membrane. Mannose pretreatment of RK13 host cells decreased their infection by *Encephalitozoon hellem*, consistent with an interaction between the mannosylation of PTP1 and some unknown host cell mannose-binding molecule (Xu et al. 2004). A CHO cell line (Lec1) that is unable to synthesize complex-type N-linked oligosaccharides and produces increased mannose-rich homogeneous $(GlcNAc)_2(Man)_5$ and O-linked fucose glycoforms had an increased susceptibility to *Encephalitozoon hellem* infection compared to wild-type CHO cells (Xu et al. 2004).

8.7 Interactions of the PTPs, SWPs, and Sporoplasm

The infection of microsporidia to the host cells is a unique, highly specialized invasion process that involves the spore wall (SW), polar tube (PT), and infectious sporoplasm (SP). Before germination, the polar tube coils inside the spore and connects to a mushroom-shaped anchoring disk (AD) at the anterior end of the spore (Vavra 1976). Upon appropriate environmental stimulation, the polar tube will discharge from the apical end of the spore, and the sporoplasm will flow through the hollow tube and appear as a droplet at the distal end (Fig. 8.11a, b) (Ohshima 1937; Han et al. 2017). Interactions between PTPs and SWPs are probably important in the polar tube orderly orientation, arrangement, and anchorage to anchoring disk and support the structural integrity of the spore wall.

Eight spore wall proteins have been identified from the Encephalitozoonidae. *Encephalitozoon cuniculi* spore wall protein 1 (EcSWP1), *Encephalitozoon intestinalis* spore wall protein 1 (EiSWP1), and EiSWP2 are localized to exospore, and *Encephalitozoon cuniculi* endospore wall protein 1 (EcEnP1), EiEnP1, EcEnP2, EcSWP3, and *Encephalitozoon cuniculi* chitin deacetylase (EcCDA) were found to be endosporal proteins (Southern et al. 2007; Peuvel-Fanget et al. 2006; Bohne et al. 2000; Brosson et al. 2005; Hayman et al. 2001; Xu et al. 2006). Ten spore wall proteins (NbSWP5, NbSWP7, NbSWP9, NbSWP11, NbSWP12, NbSWP16, NbSWP25, NbSWP26, NbSWP30, and NbSWP32) were identified by proteomic analysis from *Nosema bombycis* (Wu et al. 2008; Li et al. 2012; Yang et al. 2014, 2017; Wang et al. 2015; Chen et al. 2013; Wu et al. 2009; Li et al. 2009). Immunostaining indicated that NbSWP5, NbSWP7, and NbSWP9 localize to the spore wall and polar tube region (Yang et al. 2017; Li et al. 2012). Co-immunoprecipitation, liquid chromatography-tandem mass spectrometry, and yeast two-hybrid data revealed that NbSWP5 could interact with NbPTP2 and NbPTP3, while NbSWP9 could interact with NbPTP1 and NbPTP2 (Yang et al. 2017; Li et al. 2012). NbSWP7 may bind to the polar tube via the interaction with NbSWP9. NbSWP9 is a scaffolding protein which contributes to the anchoring of the polar tube to the spore wall (Yang et al. 2017). Several of these various SWPs are modified by posttranslational glycosylation involving mannosylation, and these modifications are probably important for spore adherence to mucin or host cells during passage of spores in the gastrointestinal tract, facilitating invasion; in support of this concept, exogenous glycosaminoglycans decreased adherence of spores to host cells (Dolgikh et al. 2007; Peuvel-Fanget et al. 2006; Hayman et al. 2005; Southern et al. 2007; Cai et al. 2011; Wu et al. 2008, 2009; Li et al. 2009; Zhu et al. 2013). SWPs may also bind to the host cell directly, and this may facilitate

invasion, e.g., NbSWP26 has been shown to bind to the turtle-like protein of *Bombycis mori* (BmTLP) (Zhu et al. 2013). Ricin-B lectin-like proteins, which in *Nosema bombycis* were found to increase infection when added to cell cultures (Liu et al. 2016), are also encoded in the genomes of other microsporidian species (Szumowski and Troemel 2015) and probably interact with carbohydrates found on host proteins facilitating spore binding.

Once polar tube germination is triggered, transportation of the sporoplasm through the polar tube is initiated when the tube has reaches ~50% extension (Jaroenlak et al. 2020). The sporoplasm then appears as a droplet at the distal end of the polar tube and remains attached to the polar tube for several minutes (Weidner 1972). Interactions between PTPs and the sporoplasm during transportation through the polar tube remain to be defined. A study utilizing correlative light and electron microscopy (CLEM) demonstrated that the droplet of released sporoplasm was still attached to the tip of polar tube during passage (Fig. 8.11a, b) (Han et al. 2017). Further study on the interactions of the polar tube and sporoplasm using yeast two-hybrid methods revealed that PTP4, which has a unique protein epitope exposed at the tip of polar tube (Han et al. 2017), could interact with sporoplasm surface protein 1 (SSP1) (Han et al. 2019). The interaction between PTP4 and SSP1 might be important as an anchor that helps to keep the sporoplasm attached to the end of polar tube after spore germination (Han et al. 2019). This interaction may be also be involved in the ability of the polar tube to coil around the sporoplasm within the intact spore, thereby establishing an anchor point for an interaction of the polar tube with the sporoplasm membrane (Han et al. 2019).

During microsporidian invasion of its host cells, EhSSP1 binds to the host cell surface at the site where the polar tube pushes into the host cell membrane (Han et al. 2019). Host cell voltage-dependent anion channels (VDAC1, VDAC2, and VDAC3) have been shown to interact with EhSSP1, and EhSSP1 co-localized with host mitochondria and the microsporidian parasitophorous vacuoles in infected cells (Han et al. 2019). Electron microscopy demonstrated that mitochondria clustered around meronts, that the outer mitochondrial membrane interacted with meronts and the parasitophorous vacuole membrane, and that VDACs were concentrated at the interface of mitochondria and parasite (Han et al. 2019). RNAi knockdown of VDAC1, VDAC2, and VDAC3 in host cells resulted in a significant decrease in the number and size of parasitophorous vacuoles and a decrease in mitochondrial parasitophorous vacuole association (Han et al. 2019). The interaction of EhSSP1 with VDAC probably plays an important part in energy acquisition by microsporidia as they lack mitochondria and are reliant on the host for ATP generation (Goldberg et al. 2008; Williams et al. 2002; Tamim El Jarkass and Reinke 2020).

8.8 The Role of the Interaction of PTPs with the Host Cell During Infection

The polar tube as the unique invasion organelle of microsporidia is the key to the success of these obligate intracellular pathogens. Despite the identification of several PTPs in the last few years, how the polar tube interacts with host cell during infection is still widely unknown. Studies on PTP1 revealed that glycosylation of PTP1 might be functional in the parasite-host interaction by creating a “sticky” polar tube capable of adhering to the host cell membrane mannose receptors (Bouzahzah and Weiss 2010; Han et al. 2020). A recent

study on the PTP4 in *Encephalitozoon hellem* identified a monoclonal antibody (mAb) which recognized an epitope of PTP4 that was exposed only at the distal end of the polar tube. Immunoprecipitation using this PTP4 mAb identified transferrin receptor 1 (TfR1), a host cell surface protein, as the potential interaction target of PTP4 during microsporidian invasion of host cells (Fig. 8.12). An interaction of PTP4 and TfR1 was further confirmed by a fluorescence co-localization assay. Alterations of the interaction between PTP4 and TfR1 either by an antibody blocking assay or by knocking out *tfr1* in host cells could significantly inhibit infection of host cells by microsporidia. These experiments suggest that for the Encephalitozoonidae (and possibly other microsporidia) PTP4 plays a crucial role in the process of invasion by interacting with host cell TfR1 (Han et al. 2017). NbPTP6 has also been shown to bind to the host cell surface, suggesting a potential role for PTP6 in the process of polar tube interaction with host cells (Lv et al. 2020).

It had been postulated that the polar tube functions like a hypodermic needle in penetration of the host cell (Weiss and Bechnel 2014; Han et al. 2020; Xu and Weiss 2005); however, electron micrographs of the polar tube interaction with its host cell demonstrated that an invagination occurs at the site of this interaction (Weiss and Bechnel 2014; Han et al. 2020). When spores are germinated in media, the sporoplasm that emerges from the polar tube tip is very delicate, swells, and breaks, suggesting that survival of the emerging sporoplasm requires a protected environment (Weiss and Bechnel 2014). It is thought that the polar tube invaginates the host cell membrane forming a microenvironment (the invasion synapse) in which final penetration occurs (Fig. 8.12). During infection, the sporoplasm is discharged from the spore through the polar tube into this invasion synapse formed by polar tube and host cell plasma membrane (Han et al. 2020). Interactions of sporoplasm surface proteins and PTPs with the host cell membrane probably occur in this invasion synapse and are likely involved in invasion, e.g., PTP4 binding to TfR1 (Han et al. 2017) and recombinant EhSSP1 has been demonstrated to bind to the host cell surface at the site where the polar tube invaginated the host cell membrane during invasion (Han et al. 2019). An ultrastructural study of *Anncaliia algerae* demonstrated that the extracellular discharged sporoplasm tightly abutted to the host plasmalemma and appeared to be in the process of being incorporated into the host cytoplasm by phagocytosis and/or endocytosis (Takvorian et al. 2005).

8.9 PTPs as Diagnostic and Genotyping Targets for Microsporidia

Microsporidia can parasitize a wide host range from invertebrates to vertebrates and have caused significant threats to human health and agricultural economic losses (Han and Weiss 2017; Stentiford et al. 2016b). The diagnosis of microsporidiosis usually involves the identification of spores in clinical samples using light microscopy employing stains such as chromotrope 2R, Calcofluor white (fluorescent brightener 28), and Uvitex 2B; however, these techniques do not identify the species of microsporidia causing an infection (van Gool et al. 1993; Vavra et al. 1992; Weber et al. 1992). Electron microscopy and molecular techniques can be used to identify the species of microsporidia causing an infection (Procop 2007). In general, molecular techniques are faster, more sensitive, and specific when compared with regular diagnostic methods for microsporidiosis (Procop 2007). Each of these detection methods has limitations: light microscopy depends on the professional skill and subjective judgment of technicians; electron microscopy is expensive, time-consuming,

and unavailable for routine diagnosis at all laboratories (Thellier and Breton 2008); and molecular techniques such as loop-mediated isothermal amplification (LAMP), nested PCR, and qPCR while highly sensitive can produce nonspecific amplicons and false-positive results if an inappropriate diagnostic target is used (Suebsing et al. 2013; Jaroenlak et al. 2016).

PTP2 has been identified in many species of microsporidia including *Encephalitozoon cuniculi*, *Encephalitozoon intestinalis*, *Encephalitozoon hellem*, *Nosema ceranae*, *Nosema bombycis*, *Paranosema grylli*, and *Enterocytozoon hepatopenaei* (Polonais et al. 2005; Cornman et al. 2009; Pan et al. 2013; Kanitchinda et al. 2020). *Enterocytozoon hepatopenaei* infects Pacific white leg shrimp *Penaeus vannamei* causing growth retardation and uneven size distributions that lead to severe losses in shrimp productivity (Jaroenlak et al. 2018). The *Enterocytozoon hepatopenaei ptp2* gene shares low nucleotide sequence similarity with *ptp2* homologues from other microsporidia. A recent study on the detection of *Enterocytozoon hepatopenaei* demonstrated that *ptp2* provided high sensitivity and specificity as a target gene for assays using recombinase polymerase amplification (RPA), CRISPR-Cas12a fluorescence, and SYBR Green I fluorescence quantitative PCR methods (Kanitchinda et al. 2020; Wang et al. 2020).

Serological diagnosis using recombinant PTPs as antigens either by immunoblotting or enzyme-linked immunosorbent assay could be potential tools to evaluate the prevalence of microsporidia in populations (Xu and Weiss 2005). It was reported previously that 8% of Dutch blood donors and 5% of pregnant French women had an IgG immune response against the polar tube of *Encephalitozoon intestinalis* (Gool et al. 1997). Carbohydrate moieties of microsporidian PTP1 have been reported to be targeted by IgG in immunocompetent individuals, and these antibodies were shown to decrease the infectivity of microsporidia in vitro (Peek et al. 2005). In another report, the class-specific anti-polar tube antibodies found in healthy and HIV-infected individuals were examined using an ELISA assay (Omura et al. 2007). Interestingly, 36% of the individuals were IgM-positive, but no IgG or IgA reactions were detected (Omura et al. 2007).

Molecular tools have been developed and employed as tools for detailed epidemiologic studies of transmission of infection, sources of infection, and analysis of subtypes of microsporidian species. A series of markers such as the internal transcribed spacer (ITS) of ribosomal DNA, the polar tube protein 1 (PTP1) gene, and two intergenic spacers (IGS-TH and IGS-HZ) have been utilized for genotyping of microsporidia (Haro et al. 2003). These markers have been used to look at zoonotic transmission of various microsporidia by defining specific subtypes seen in different animals. In general, genotyping of microsporidia using ITS markers has not been used as a routine test in most diagnostic laboratories due to technical demands and high cost (Xiao et al. 2001b). The gene coding sequence of PTP1 of *Encephalitozoon cuniculi* and *Encephalitozoon hellem* has long central repeats of 78 bp and 60 bp, and these regions have been used to examine the genetic diversity of isolates of these microsporidia (Delbac et al. 1998b; Keohane et al. 1998). Nucleotide sequence analysis of the PTP1 gene divided 11 *Encephalitozoon cuniculi* isolates into 3 genotypes and 24 *Encephalitozoon cuniculi* isolates into 4 genotypes (Xiao et al. 2001a, b).

8.10 Conclusion and Future Perspectives

Microsporidia have been identified as pathogens that have important effects on our health, food security, and economy (Stentiford et al. 2016b). Human microsporidiosis represents a significant emerging opportunistic disease, once thought to be restricted to immune-compromised patients; however, infections in immune-competent individuals also occur (Sak et al. 2011; Didier and Weiss 2011). The polar tube is part of the unique invasion organelle of microsporidia which plays a critical role during microsporidia infection. Despite its description over 125 years ago by Thelohan (Thelohan 1894), we still do not understand the details of how this structure functions and the exact mechanism by which microsporidia enter their host cells and establish a host-pathogen relationship. Progress, however, has been made in understanding the proteins in this invasion apparatus and the interaction of these proteins with some host cell proteins. Understanding how microsporidia use host cell proteins in both invasion and egress will provide insight into their impact on hosts and enhance our current understanding of the transmission dynamics of these pathogens. Due to the importance of various PTPs such as PTP1 and PTP4 in the invasion process, drugs or antibodies which could inhibit the interaction of PTPs with host proteins should provide information needed for new therapeutic approaches to control these pathogens.

Acknowledgments

All of the standard transmission electron microscopy (TEM) was conducted at the Rutgers Newark Electron Microscopy Facility which was funded in part by NIH grant AI091985 awarded to Dr. Ann Cali. Some of the cryo-TEM microscopy was conducted at the Albert Einstein Analytical Imaging Facility (AECOM) which is supported in part by the NCI Cancer Center Support GrantP30CA013330 and shared instrumentation grant 1S10OD016214–01A1. Additional CTEM and the focused ion beam scanning electron microscopy (FIB-SEM) were performed at the Simons Electron Microscopy Center and National Resource for Automated Molecular Microscopy located at the New York Structural Biology Center (NYSBC), supported by grants from the Simons Foundation (SF349247), NYSTAR, and the NIH National Institute of General Medical Sciences (GM103310). We also thank William Rice for his assistance with the CTEM and FIB-SEM and Ashleigh Raczkowski NYSBC. Additionally, we thank Xheni Nishku AECOM for her assistance with the segmentation and 3-D images. PMT would like to thank Dr. Ann Cali for her many discussions and insightful ideas and for sharing her bountiful knowledge on the microsporidia.

Funding

This work was supported by the National Institutes of Health/National Institute of Allergy and Infectious Diseases grants AI124753 (L.M.W.) and AI132614 (L.M.W.), the National Natural Science Foundation of China (grant no. 32000106) (B.H.), and the QILU Young Scholars Program of Shandong University (grant no. 21510082063092) (B.H.).

References

Aurrecoechea C, Barreto A, Brestelli J, Brunk BP, Caler EV, Fischer S, Gajria B, Gao X, Gingle A, Grant G, Harb OS, Heiges M, Iodice J, Kissinger JC, Kraemer ET, Li W, Nayak V, Pennington C, Pinney DF, Pitts B, Roos DS, Srinivasamoorthy G, Stoeckert CJ Jr, Treatman C, Wang H (2011) AmoebaDB and MicrosporidiaDB: functional genomic resources for Amoebozoa and microsporidia species. Nucleic Acids Res 39(Database Issue):D612–D619. 10.1093/nar/gkq1006 [PubMed: 20974635]

Beznoussenko GV, Dolgikh VV, Seliverstova EV, Semenov PB, Tokarev YS, Trucco A, Micaroni M, Di Giandomenico D, Auinger P, Senderskiy IV, Skarlato SO, Snigirevskaya ES, Komissarchik YY, Pavelka M, De Matteis MA, Luini A, Sokolova YY, Mironov AA (2007) Analogs of the Golgi complex in microsporidia: structure and avesicular mechanisms of function. J Cell Sci 120(Pt 7):1288–1298. 10.1242/jcs.03402 [PubMed: 17356068]

Bohne W, Ferguson DJ, Kohler K, Gross U (2000) Developmental expression of a tandemly repeated, glycine-and serine-rich spore wall protein in the microsporidian pathogen Encephalitozoon cuniculi. Infect Immun 68(4):2268–2275 [PubMed: 10722629]

Bouzahzah B, Weiss LM (2010) Glycosylation of the major polar tube protein of Encephalitozoon cuniculi. Parasitol Res 107(3):761–764. 10.1007/s00436-010-1950-7 [PubMed: 20556427]

Bouzahzah B, Nagajyothi F, Ghosh K, Takvorian PM, Cali A, Tanowitz HB, Weiss LM (2010) Interactions of Encephalitozoon cuniculi polar tube proteins. Infect Immun 78(6):2745–2753. 10.1128/IAI.01205-09 [PubMed: 20308291]

Brosson D, Kuhn L, Prensier G, Vivares CP, Texier C (2005) The putative chitin deacetylase of Encephalitozoon cuniculi: a surface protein implicated in microsporidian spore-wall formation. FEMS Microbiol Lett 247(1):81–90 [PubMed: 15927751]

Cai S, Lu X, Qiu H, Li M, Feng Z (2011) Identification of a Nosema bombycis (microsporidia) spore wall protein corresponding to spore phagocytosis. Parasitology 138(9):1102–1109. 10.1017/S0031182011000801 [PubMed: 21756420]

Cali A, Takvorian PM (2014) Developmental morphology and life cycles of the microsporidia. In: Microsporidia, pp 71–133. 10.1002/9781118395264.ch2

Cali A, Weiss LM, Takvorian PM (2002) Brachiola algerae spore membrane systems, their activity during extrusion, and a new structural entity, the multilayered interlaced network, associated with the polar tube and the sporoplasm. J Eukaryot Microbiol 49(2):164–174. 10.1111/j.1550-7408.2002.tb00361.x [PubMed: 12043963]

Chen J, Geng L, Long M, Li T, Li Z, Yang D, Ma C, Wu H, Ma Z, Li C (2013) Identification of a novel chitin-binding spore wall protein (NbSWP12) with a BAR-2 domain from Nosema bombycis (microsporidia). Parasitology 140(11):1394–1402 [PubMed: 23920053]

Chioralia G, Trammer T, Maier WA, Seitz HM (1998) Morphologic changes in Nosema algerae (Microspora) during extrusion. Parasitol Res 84(2):123–131. 10.1007/s004360050368 [PubMed: 9493211]

Cornman RS, Chen YP, Schatz MC, Street C, Zhao Y, Desany B, Egholm M, Hutchison S, Pettis JS, Lipkin WI (2009) Genomic analyses of the microsporidian Nosema ceranae, an emergent pathogen of honey bees. PLoS Pathog 5(6):e1000466 [PubMed: 19503607]

Delbac F, Duffieux F, David D, Metenier G, Vivares CP (1998a) Immunocytochemical identification of spore proteins in two microsporidia, with emphasis on extrusion apparatus. J Eukaryot Microbiol 45(2):224–231 [PubMed: 9561775]

Delbac F, Peyret P, Metenier G, David D, Danchin A, Vivares CP (1998b) On proteins of the microsporidian invasive apparatus: complete sequence of a polar tube protein of Encephalitozoon cuniculi. Mol Microbiol 29(3):825–834 [PubMed: 9723921]

Delbac F, Peuvel I, Metenier G, Peyretaillade E, Vivares CP (2001) Microsporidian invasion apparatus: identification of a novel polar tube protein and evidence for clustering of ptp1 and ptp2 genes in three Encephalitozoon species. Infect Immun 69(2):1016–1024 [PubMed: 11159998]

Desportes-Livage I, Datry A (2005) Infections à microsporidies, Isospora et Sarcocystis. EMC - Maladies Infectieuses 2(4):178–196. 10.1016/j.emcmi.2005.08.001

Didier ES, Weiss LM (2011) Microsporidiosis: not just in AIDS patients. Curr Opin Infect Dis 24(5):490 [PubMed: 21844802]

Dolgikh VV, Semenov PB, Mironov AA, Beznoussenko GV (2005) Immunocytochemical identification of the major exospore protein and three polar-tube proteins of the microsporidia Paranosema grylli. Protist 156(1):77–87 [PubMed: 16048134]

Dolgikh VV, Semenov PB, Beznusenko GV (2007) Protein glycosylation in the spores of the microsporidia Paranosema (Antonospora) grylli. Tsitologiia 49(7):607–613 [PubMed: 17918346]

Frixione E, Ruiz L, Santillan M, Devargas LV, Tejero JM, Undeen AH (1992) Dynamics of polar filament discharge and Sporoplasm expulsion by microsporidian spores. Cell Motil Cytoskel 22(1):38–50. 10.1002/cm.970220105

Goldberg AV, Molik S, Tsaousis AD, Neumann K, Kuhnke G, Delbac F, Vivares CP, Hirt RP, Lill R, Embley TM (2008) Localization and functionality of microsporidian iron–Sulphur cluster assembly proteins. Nature 452(7187):624–628 [PubMed: 18311129]

Gool TV, Vetter JCM, Weinmayr B, Dam AV, Derouin F, Dankert J (1997) High seroprevalence of Encephalitozoon species in immunocompetent subjects. J Infect Dis 175(4):1020–1024 [PubMed: 9086174]

Han B, Weiss LM (2017) Microsporidia: obligate intracellular pathogens within the fungal kingdom. Microbiol Spectr 5(2). 10.1128/microbiolspec.FUNK-0018-2016

Han B, Polonais V, Sugi T, Yakubu R, Takvorian PM, Cali A, Maier K, Long M, Levy M, Tanowitz HB, Pan G, Delbac F, Zhou Z, Weiss LM (2017) The role of microsporidian polar tube protein 4 (PTP4) in host cell infection. PLoS Pathog 13(4):e1006341. 10.1371/journal.ppat.1006341PPATHOGENS-D-16-01789. [pii] [PubMed: 28426751]

Han B, Ma Y, Tu V, Tomita T, Mayoral J, Williams T, Horta A, Huang H, Weiss LM (2019) Microsporidia interact with host cell mitochondria via voltage-dependent anion channels using sporoplasm surface protein 1. mBio 10(4):e01944–e01919. 10.1128/mBio.01944-19 [PubMed: 31431557]

Han B, Takvorian PM, Weiss LM (2020) Invasion of host cells by microsporidia. Front Microbiol 11(172):1–16. 10.3389/fmicb.2020.00172 [PubMed: 32082274]

Han B, Pan G, Weiss LM (2021) Microsporidiosis in humans. Clin Microbiol Rev 34(4):e0001020. 10.1128/CMR.00010-20

Haro M, Del Aguila C, Fenoy S, Henriques-Gil N (2003) Intraspecies genotype variability of the microsporidian parasite Encephalitozoon hellem. J Clin Microbiol 41(9):4166–4171. 10.1128/jcm.41.9.4166-4171.2003 [PubMed: 12958242]

Haro M, Izquierdo F, Henriques-Gil N, Andrés I, Alonso F, Fenoy S, del Águila C (2005) First detection and genotyping of human-associated microsporidia in pigeons from urban parks. Appl Environ Microbiol 71(6):3153. 10.1128/AEM.71.6.3153-3157.2005 [PubMed: 15933015]

Hayman JR, Hayes SF, Amon J, Nash TE (2001) Developmental expression of two spore wall proteins during maturation of the microsporidian Encephalitozoon intestinalis. Infect Immun 69(11):7057–7066 [PubMed: 11598081]

Hayman JR, Southern TR, Nash TE (2005) Role of sulfated glycans in adherence of the microsporidian Encephalitozoon intestinalis to host cells in vitro. Infect Immun 73(2):841–848 [PubMed: 15664924]

Huger A (1960) Electron microscope study on the cytology of a microsporidian spore by means of ultrathin sectioning. J Insect Pathol 2:84–105

James TY, Pelin A, Bonen L, Ahrendt S, Sain D, Corradi N, Stajich JE (2013) Shared signatures of parasitism and phylogenomics unite Cryptomycota and microsporidia. Curr Biol 23(16): 1548–1553. 10.1016/j.cub.2013.06.057 [PubMed: 23932404]

Jaroenlak P, Sanguanrut P, Williams BAP, Stentiford GD, Flegel TW, Sritunyalucksana K, Itsathitphaisarn O (2016) A nested PCR assay to avoid false positive detection of the microsporidian enterocytozoon hepatopenaei (EHP) in environmental samples in shrimp farms. PLoS One 11(11). 10.1371/JOURNAL.PONE.0166320

Jaroenlak P, Boakye DW, Vanichviriyakit R, Williams BA, Sritunyalucksana K, Itsathitphaisarn O (2018) Identification, characterization and heparin binding capacity of a spore-wall, virulence protein from the shrimp microsporidian, Enterocytozoon hepatopenaei (EHP). Parasit Vectors 11(1):177 [PubMed: 29530076]

Jaroenlak P, Cammer M, Davydov A, Sall J, Usmani M, Liang FX, Ekiert DC, Bhabha G (2020) 3-dimensional organization and dynamics of the microsporidian polar tube invasion machinery. PLoS Pathog 16(9):e1008738. 10.1371/journal.ppat.1008738 [PubMed: 32946515]

Juarez S, Putaporntip C, Jongwutiwes S, Ichinose A, Yanagi T, Kanbara H (2005) In vitro cultivation and electron microscopy characterization of Trachipleistophora anthropophthera isolated from the cornea of an AIDS patient. J Eukaryot Microbiol 52:179–190. 10.1111/j.1550-7408.2005.00024.x [PubMed: 15926993]

Kanitchinda S, Srisala J, Suebsing R, Prachumwat A, Chaijarasphong T (2020) CRISPR-Cas fluorescent cleavage assay coupled with recombinase polymerase amplification for sensitive and specific detection of Enterocytozoon hepatopenaei. Biotechnol Rep 27:e00485. 10.1016/J.BTRE.2020.E00485

Katinka MD, Duprat S, Cornillot E, Metenier G, Thomarat F, Prensier G, Barbe V, Peyretaillade E, Brottier P, Wincker P, Delbac F, El Alaoui H, Peyret P, Saurin W, Gouy M, Weissenbach J, Vivares CP (2001) Genome sequence and gene compaction of the eukaryote parasite Encephalitozoon cuniculi. Nature 414(6862):450–453 [PubMed: 11719806]

Keohane EM, Weiss LM (1998) Characterization and function of the microsporidian polar tube: a review. Folia Parasitol 45(2):117–127

Keohane E, Weiss LM (1999) The structure, function, and composition of the microsporidian polar tube. In: Wittner M, Weiss LM (eds) The Microsporidia and Microsporidiosis. ASM Press, Washington, DC, pp 196–224

Keohane E, Takvorian PM, Cali A, Tanowitz HB, Wittner M, Weiss LM (1994) The identification and characterization of a polar tube reactive monoclonal antibody. J Eukaryot Microbiol 41(5): 48S [PubMed: 7804249]

Keohane EM, Orr GA, Takvorian PM, Cali A, Tanowitz HB, Wittner M, Weiss LM (1996a) Purification and characterization of a microsporidian polar tube proteins. J Eukaryot Microbiol 43(5):100S [PubMed: 8822888]

Keohane EM, Orr GA, Takvorian PM, Cali A, Tanowitz HB, Wittner M, Weiss LM (1996b) Identification of a microsporidian polar tube reactive monoclonal antibody. J Euk Micobiol 43(1):26–31

Keohane EM, Takvorian PM, Cali A, Tanowitz HB, Wittner M, Weiss LM (1996c) Identification of a microsporidian polar tube protein reactive monoclonal antibody. J Eukaryot Microbiol 43(1): 26–31 [PubMed: 8563706]

Keohane EM, Orr GA, Zhang HS, Takvorian PM, Cali A, Tanowitz HB, Wittner M, Weiss LM (1998) The molecular characterization of the major polar tube protein gene from Encephalitozoon hellem, a microsporidian parasite of humans. Mol Biochem Parasitol 94(2): 227–236 [PubMed: 9747973]

Keohane EM, Orr GA, Takvorian PM, Cali A, Tanowitz HB, Wittner M, Weiss LM (1999) Analysis of the major microsporidian polar tube proteins. J Eukaryot Microbiol 46(5):29S–30S [PubMed: 10519234]

Kramer JP (1960) Observations on the emergence of the microsporidian sporoplasm. J Insect Pathol 2:433–439

Li Y, Wu Z, Pan G, He W, Zhang R, Hu J, Zhou Z (2009) Identification of a novel spore wall protein (SWP26) from microsporidia Nosema bombycis. Int J Parasitol 39(4):391–398. 10.1016/j.ijpara.2008.08.011 [PubMed: 18854188]

Li Z, Pan G, Li T, Huang W, Chen J, Geng L, Yang D, Wang L, Zhou Z (2012) SWP5, a spore wall protein, interacts with polar tube proteins in the parasitic microsporidian Nosema bombycis. Eukaryot Cell 11(2):229–237. 10.1128/EC.05127-11 [PubMed: 22140229]

Liu H, Li M, Cai S, He X, Shao Y, Lu X (2016) Ricin-B-lectin enhances microsporidia Nosema bombycis infection in BmN cells from silkworm Bombyx mori. Acta Biochim Biophys Sin Shanghai 48(11):1050–1057. 10.1093/abbs/gmw093 [PubMed: 27649890]

Lom J, Vavra J (1963) The mode of sporoplasm extrusion in microsporidian spores. Acta Protozool 1:81–89

Lussier M, Sdicu AM, Bussereau F, Jacquet M, Bussey H (1997) The Ktr1p, Ktr3p, and Kre2p/ Mnt1p mannosyltransferases participate in the elaboration of yeast O- and N-linked carbohydrate chains. J Biol Chem 272(24):15527–15531. 10.1074/jbc.272.24.15527 [PubMed: 9182588]

Lv Q, Wang L, Fan Y, Meng X, Liu K, Zhou B, Chen J, Pan G, Long M, Zhou Z (2020) Identification and characterization a novel polar tube protein (NbPTP6) from the microsporidian Nosema bombycis. Parasit Vectors 13(1):475. 10.1186/s13071-020-04348-z [PubMed: 32933572]

Moss JA, Snyder RA (2017) Biofilms for monitoring presence of microsporidia in environmental water. J Eukaryot Microbiol 64(4):533–538. 10.1111/jeu.12390 [PubMed: 27995672]

Ohshima K (1937) On the function of the polar filament of Nosema bombycis. Parasitology 29(02): 220–224

Omura M, Furuya K, Kudo S, Sugiura W, Azuma H (2007) Detecting immunoglobulin M antibodies against microsporidian Encephalitozoon cuniculi polar tubes in sera from healthy and human immunodeficiency virus-infected persons in Japan. Clin Vaccine Immunol 14(2): 168–172. 10.1128/CVI.00224-06 [PubMed: 17108286]

Orlandi PA, Chu D-MT, Bier JW, Jackson GJ (2002) Parasites and the food supply. Food Technology-Champaign Then Chicago 56(4):72–79

Pan GQ, Xu JS, Li T, Xia QY, Liu SL, Zhang GJ, Li SG, Li CF, Liu HD, Yang L, Liu T, Zhang X, Wu ZL, Fan W, Dang XQ, Xiang H, Tao ML, Li YH, Hu JH, Li Z, Lin LP, Luo J, Geng LN, Wang LL, Long MX, Wan YJ, He NJ, Zhang Z, Lu C, Keeling PJ, Wang J, Xiang ZH, Zhou ZY (2013) Comparative genomics of parasitic silkworm microsporidia reveal an association between genome expansion and host adaptation. BMC Genomics 14:186. 10.1186/1471-2164-14-186 [PubMed: 23496955]

Paterson RRM, Lima N (2015) Molecular biology of food and water borne Mycotoxigenic and mycotic fungi. CRC Press, Boca Raton

Peek R, Delbac F, Speijer D, Polonais V, Greve S, Wentink-Bonnema E, Ringrose J, van Gool T (2005) Carbohydrate moieties of microsporidian polar tube proteins are targeted by immuno-globulin G in immunocompetent individuals. Infect Immun 73(12):7906–7913 [PubMed: 16299281]

Peuvel I (2000) Polymorphism of the gene encoding a major polar tube protein PTP1 in two microsporidia of the genus Encephalitozoon. Parasitology 121(6):581 [PubMed: 11155928]

Peuvel I, Peyret P, Metenier G, Vivares CP, Delbac F (2002) The microsporidian polar tube: evidence for a third polar tube protein (PTP3) in Encephalitozoon cuniculi. Mol Biochem Parasitol 122(1):69–80 [PubMed: 12076771]

Peuvel-Fanget I, Polonais V, Brosson D, Texier C, Kuhn L, Peyret P, Vivares C, Delbac F (2006) EnP1 and EnP2, two proteins associated with the Encephalitozoon cuniculi endospore, the chitin-rich inner layer of the microsporidian spore wall. Int J Parasitol 36(3):309–318 [PubMed: 16368098]

Polonais V, Prensier G, Méténier G, Vivarès CP, Delbac F (2005) Microsporidian polar tube proteins: highly divergent but closely linked genes encode PTP1 and PTP2 in members of the evolutionarily distant Antonospora and Encephalitozoon groups. Fungal Genet Biol 42(9): 791–803 [PubMed: 16051504]

Polonais V, Belkorchia A, Roussel M, Peyretaillade E, Peyret P, Diogon M, Delbac F (2013) Identification of two new polar tube proteins related to polar tube protein 2 in the microsporidian Antonospora locustae. FEMS Microbiol Lett 346(1):36–44. 10.1111/1574-6968.12198 [PubMed: 23763358]

Procop GW (2007) Molecular diagnostics for the detection and characterization of microbial pathogens. Clin Infect Dis 45(Supplement_2):S99–S111 [PubMed: 17683022]

Ramanan P, Pritt BS (2014) Extraintestinal Microsporidiosis. J Clin Microbiol 52(11):3839–3844. 10.1128/jcm.00971-14 [PubMed: 24829239]

Sak B, Brady D, Pelikánová M, Květoňová D, Rost M, Kostka M, Tolarová V, Hůzová Z, Kváč M (2011) Unapparent microsporidial infection among immunocompetent humans in the Czech Republic. J Clin Microbiol 49(3):1064–1070. 10.1128/jcm.01147-10 [PubMed: 21191056]

Southern TR, Jolly CE, Lester ME, Hayman JR (2007) EnP1, a microsporidian spore wall protein that enables spores to adhere to and infect host cells in vitro. Eukaryot Cell 6(8):1354–1362 [PubMed: 17557882]

Stentiford G, Becnel J, Weiss L, Keeling P, Didier E, Williams B, Bjornson S, Kent M, Freeman M, Brown M (2016a) Microsporidia–emergent pathogens in the global food chain. Trends Parasitol 32(4):336–348 [PubMed: 26796229]

Stentiford GD, Becnel J, Weiss LM, Keeling PJ, Didier ES, Williams BP, Bjornson S, Kent ML, Freeman MA, Brown MJF, Troemel ER, Roesel K, Sokolova Y, Snowden KF, Solter L (2016b) Microsporidia - emergent pathogens in the global food chain. Trends Parasitol 32(4):336–348. 10.1016/j.pt.2015.12.004 [PubMed: 26796229]

Suebsing R, Prombun P, Srisala J, Kiatpathomchai W (2013) Loop-mediated isothermal amplification combined with colorimetric nanogold for detection of the microsporidian Enterocytozoon hepatopenaei in penaeid shrimp. J Appl Microbiol 114(5):1254–1263. 10.1111/JAM.12160 [PubMed: 23387348]

Szumowski SC, Troemel ER (2015) Microsporidia-host interactions. Curr Opin Microbiol 26:10–16. 10.1016/j.mib.2015.03.006 [PubMed: 25847674]

Takvorian PM, Cali A (1986) The ultrastructure of spores (protozoa: Microsporida) from Lophius americanus, the angler fish. J Protozool 33(4):570–575. 10.1111/j.1550-7408.1986.tb05664.x [PubMed: 3795144]

Takvorian PM, Cali A (1994) Enzyme-histochemical identification of the Golgi-apparatus in the microsporidian, Glugea-Stephani. J Eukaryot Microbiol 41(5):S63–S64

Takvorian PM, Cali A (1996) Polar tube formation and nucleoside diphosphatase activity in the microsporidian, Glugea stephani. J Eukaryot Microbiol 43(5):S102–S103. 10.1111/j.1550-7408.1996.tb05025.x

Takvorian PM, Weiss LM, Cali A (2005) The early events of Brachiola algerae (microsporidia) infection: spore germination, sporoplasm structure, and development within host cells. Folia Parasitol 52(1–2):118–129

Takvorian PM, Han B, Cali A, Rice WJ, Gunther L, Macaluso F, Weiss LM (2020) An ultrastructural study of the extruded polar tube of Anncaliia algerae (microsporidia). J Eukaryot Microbiol 67(1):28–44. 10.1111/jeu.12751 [PubMed: 31332877]

Tamim El Jarkass H, Reinke AW (2020) The ins and outs of host-microsporidia interactions during invasion, proliferation and exit. Cell Microbiol 22(11):e13247. 10.1111/cmi.13247 [PubMed: 32748538]

Thellier M, Breton J (2008) Enterocytozoon bieneusi in human and animals, focus on laboratory identification and molecular epidemiology. Parasite 15(3):349–358. 10.1051/parasite/2008153349 [PubMed: 18814706]

Thelohan P (1894) Sur la presence d'une capsule a filament dans les spores des microsporidies. CR Acad Sci 118:1425–1427

van Gool T, Snijders F, Reiss P, Eeftinck Schattenkerk JK, van den Bergh Weerman MA, Bartelsman JF, Bruins JJ, Canning EU, Dankert J (1993) Diagnosis of intestinal and disseminated microsporidial infections in patients with HIV by a new rapid fluorescence technique. J Clin Pathol 46(8):694–699 [PubMed: 8408691]

Varki A (1993) Biological roles of oligosaccharides: all of the theories are correct. Glycobiology 3(2):97–130. 10.1093/GLYCOB/3.2.97 [PubMed: 8490246]

Vavra J (1976) Structure of the microsporidia. In: Bulla LA Jr, Cheng TC (eds) Comparative pathobiology, vol 1. Plenum Press, New York, pp 1–85

Vavra J, Dahbiova R, Hollister W, Canning E (1992) Staining of microsporidian spores by optical brighteners with remarks on the use of brighteners for the diagnosis of AIDS associated human microsporidioses. Folia Parasitol 40(4):267–272

Visvesvara GS (2002) In vitro cultivation of microsporidia of clinical importance. Clin Microbiol Rev 15(3):401–413 [PubMed: 12097248]

Wang JY, Chambon C, Lu CD, Huang KW, Vivares CP, Texier C (2007) A proteomic-based approach for the characterization of some major structural proteins involved in host-parasite relationships from the silkworm parasite Nosema bombycis (microsporidia). Proteomics 7(9): 1461–1472. 10.1002/pmic.200600825 [PubMed: 17407187]

Wang Y, Dang X, Ma Q, Liu F, Pan G, Li T, Zhou Z (2015) Characterization of a novel spore wall protein NbSWP16 with proline-rich tandem repeats from Nosema bombycis (microsporidia). Parasitology 142(4):534–542 [PubMed: 25363531]

Wang L, Lv Q, He Y, Gu R, Zhou B, Chen J, Fan X, Pan G, Long M, Zhou Z (2020) Integrated qPCR and staining methods for detection and quantification of *Enterocytozoon hepatopenaei* in Shrimp *Litopenaeus vannamei*. Microorganismsv 8:1366. 10.3390/MICROORGANISMS8091366

Weber R, Bryan RT, Owen RL, Wilcox CM, Gorelkin L, Visvesvara GS, Group EOIW (1992) Improved light-microscopal detection of microsporidia spores in stool and duodenal aspirates. New England J Med 326:161–166 [PubMed: 1370122]

Weber R, Bryan RT, Schwartz DA, Owen RL (1994) Human Microsporidial infections. Clin Microbiol Rev 7(4):426–461 [PubMed: 7834600]

Weber R, Deplazes P, Schwartz D (2000) Diagnosis and clinical aspects of human microsporidiosis. Contrib Microbiol 6:166–192 [PubMed: 10943512]

Weidner E (1972) Ultrastructural study of microsporidian invasion into cells. Z Parasitenkd 40(3): 227–242. 10.1007/BF00329623 [PubMed: 4346238]

Weidner E (1976) The microsporidian spore invasion tube. The ultrastructure, isolation, and characterization of the protein comprising the tube. J Cell Biol 71(1):23–34 [PubMed: 10309]

Weiss LM (2014) Clinical syndromes associated with microsporidiosis. Microsporidia: pathogens of opportunity. Wiley-Blackwell, Oxford, pp 371–401

Weiss LM (2020) Microsporidiosis. In: Hunter's tropical medicine and emerging infectious diseases. Elsevier, Amsterdam, pp 825–831

Weiss LM, Bechnel JJ (2014) Microsporidia: pathogens of opportunity. Wiley Press, New York

Weiss LM, Vossbrinck CR (1999) Molecular biology, molecular phylogeny, and molecular diagnostic approaches to the microsporidia. In: Wittner M, Weiss LM (eds) The microsporidia and microsporidia. ASM Press, Washington, DC, pp 129–171

Weiss LM, Delbac F, Hayman JR, Pan G, Dang X, Zhou Z (2014) The microsporidian polar tube and Spore Wall. In: Weiss LM, Bechnel JJ (eds) Microsporidia: pathogens of opportunity. Wiley Blackwell, Oxford, pp 261–306

Williams BAP, Hirt RP, Lucocq JM, Embley TM (2002) A mitochondrial remnant in the microsporidian Trachipleistophora hominis. Nature 418:865. 10.1038/nature00949 [PubMed: 12192407]

Wu Z, Li Y, Pan G, Tan X, Hu J, Zhou Z, Xiang Z (2008) Proteomic analysis of spore wall proteins and identification of two spore wall proteins from Nosema bombycis (microsporidia). Proteomics 8(12):2447–2461. 10.1002/pmic.200700584 [PubMed: 18563739]

Wu Z, Li Y, Pan G, Zhou Z, Xiang Z (2009) SWP25, a novel protein associated with the Nosema bombycis endospore. J Eukaryot Microbiol 56(2):113–118. 10.1111/j.1550-7408.2008.00375.x [PubMed: 19457051]

Xiao L, Li L, Moura H, Sulaiman I, Lal AA, Gatti S, Scaglia M, Didier ES, Visvesvara GS (2001a) Genotyping Encephalitozoon hellem isolates by analysis of the polar tube protein gene. J Clin Microbiol 39(6):2191–2196. 10.1128/JCM.39.6.2191-2196.2001 [PubMed: 11376056]

Xiao L, Li L, Visvesvara GS, Moura H, Didier ES, Lal AA (2001b) Genotyping Encephalitozoon cuniculi by multilocus analyses of genes with repetitive sequences. J Clin Microbiol 39(6): 2248–2253. 10.1128/JCM.39.6.2248-2253.2001 [PubMed: 11376065]

Xu Y, Weiss LM (2005) The microsporidian polar tube: a highly specialised invasion organelle. Int J Parasitol 35(9):941–953. 10.1016/j.ijpara.2005.04.003 [PubMed: 16005007]

Xu Y, Takvorian P, Cali A, Weiss LM (2003) Lectin binding of the major polar tube protein (PTP1) and its role in invasion. J Eukaryot Microbiol 50(S1):600–601 [PubMed: 14736177]

Xu Y, Takvorian PM, Cali A, Orr G, Weiss LM (2004) Glycosylation of the major polar tube protein of Encephalitozoon hellem, a microsporidian parasite that infects humans. Infect Immun 72(11):6341–6350. 10.1128/IAI.72.11.6341-6350.2004 [PubMed: 15501763]

Xu Y, Takvorian P, Cali A, Wang F, Zhang H, Orr G, Weiss LM (2006) Identification of a new Spore Wall protein from Encephalitozoon cuniculi. Infect Immun 74(1):239–247 [PubMed: 16368977]

Yang D, Dang X, Peng P, Long M, Ma C, Qin JJG, Wu H, Liu T, Zhou X, Pan G (2014) NbHSWP11, a microsporidia Nosema bombycis protein, localizing in the spore wall and membranes, reduces spore adherence to host cell BME. J Parasitol 100(5):623–633 [PubMed: 24813020]

Yang D, Pan L, Peng P, Dang X, Li C, Li T, Long M, Chen J, Wu Y, Du H (2017) Interaction between SWP9 and PTPs of the microsporidian Nosema bombycis and SWP9 as a scaffolding protein contributes to the polar tube tethering to spore wall. Infect Immun 85(3):e00872–16 [PubMed: 28031263]

Yang D, Pan L, Chen Z, Du H, Luo B, Luo J, Pan G (2018) The roles of microsporidia spore wall proteins in the spore wall formation and polar tube anchorage to spore wall during development and infection processes. Exp Parasitol 187:93–100 [PubMed: 29522765]

Zhu F, Shen Z, Hou J, Zhang J, Geng T, Tang X, Xu L, Guo X (2013) Identification of a protein interacting with the spore wall protein SWP26 of Nosema bombycis in a cultured BmN cell line of silkworm. Infect Genet Evol 17:38–45. 10.1016/j.meegid.2013.03.029 [PubMed: 23542093]

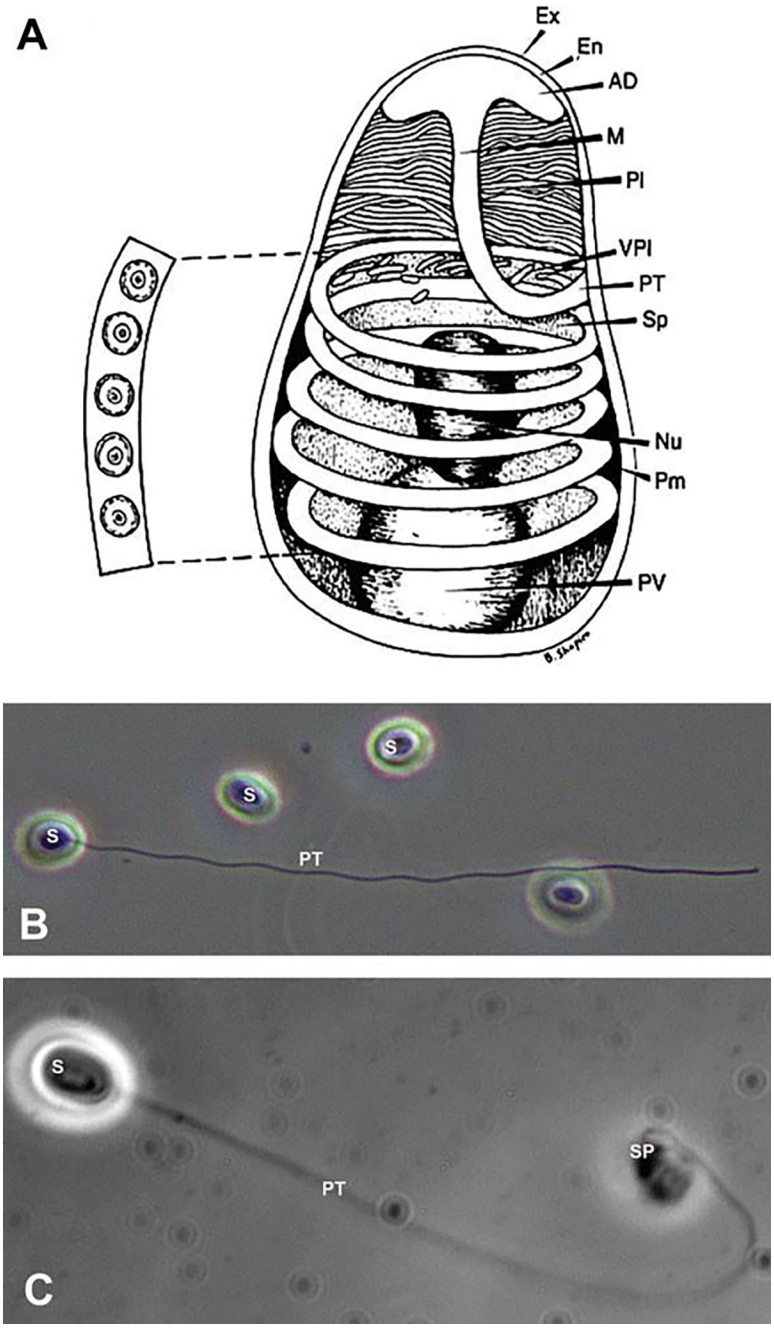

Fig. 8.1.

Microsporidian spore structure and light microscope images. (a) Diagram of a microsporidian spore. Microsporidian spores vary in size from 1 to 12 μm. The spore coat is thinner at the anterior end of the spore and consists of an electron lucent endospore (En), electron-dense exospore (Ex), and the plasma membrane (Pm). The sporoplasm (Sp) contains ribosomes, the posterior vacuole (PV), and a single nucleus (Nu). The anchoring disc (AD) at the anterior end of the spore is the site of attachment of the polar tube. It should be noted that the polar tube is often called the polar filament when it is within the spore prior to germination. The anterior or straight region of the polar tube that connects

to the anchoring disc is called the manubroid (M), and the posterior region of the tube coils around the sporoplasm. The number of coils and their arrangement (i.e., single row or multiple rows) is used in microsporidian taxonomic classification. The lamellar polaroplast (Pl) and vesicular polaroplast (VPl) surround the manubroid region of the polar tube. The insert depicts the polar tube coils in this figure in a cross section illustrating that the polar tube within the spore (i.e., polar filament) has several layers of different electron density by electron microscopy. Reprinted with permission from Keohane EM, Weiss LM. 1999. The structure, function, and composition of the microsporidian polar tube. pp. 196–224. *In* Wittner M, Weiss LM (ed), The Microsporidia and Microsporidiosis. ASM Press, Washington, DC (Keohane and Weiss 1999). (b) Differential interference contrast (DIC) microscopy image of *Anncaliia algerae* spores. One of the spores (S) has become activated, and the polar tube (PT) is in the process of extrusion. (c) Phase contrast microscopic image of an *Anncaliia algerae* spore (S) with the extruded polar tube (PT) and the sporoplasm (SPM) still attached to the distal end of the PT

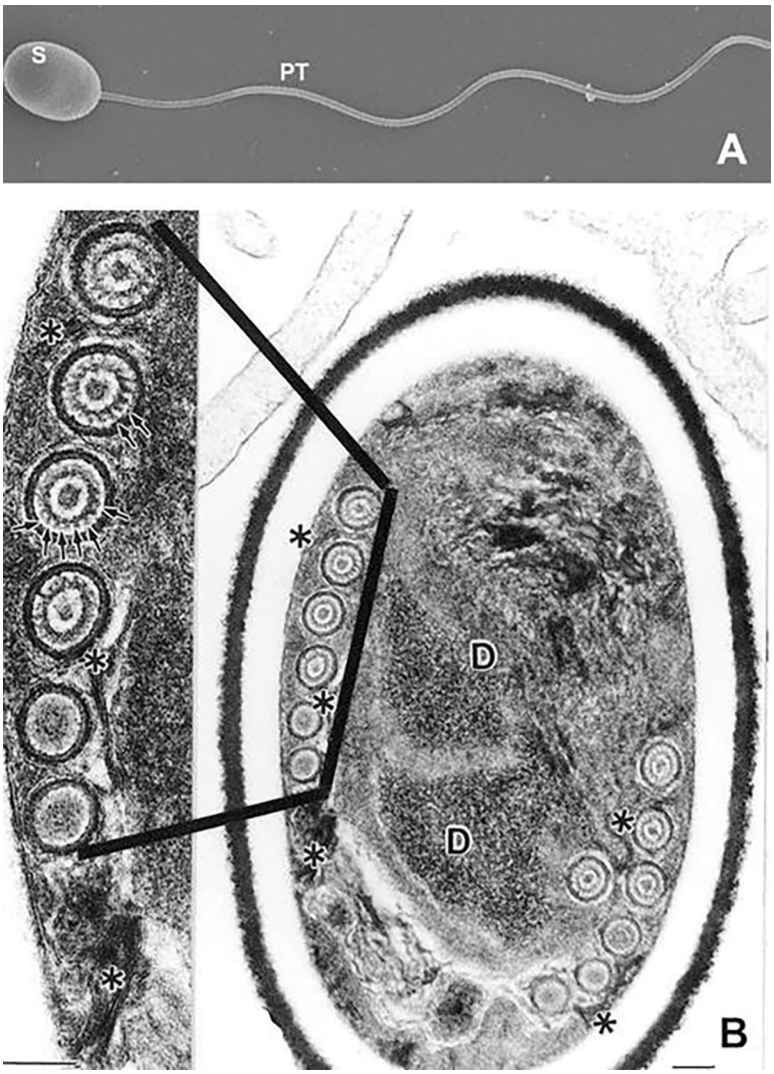

Fig. 8.2.

Scanning and transmission electron microscopic images of microsporidian spores. (a) Scanning electron microscope image of an activated *Anncaliia algerae* spore (S) with the extruded polar tube (PT). (b) Transmission electron microscope (TEM) image of an *Anncaliia algerae* spore and an enlarged image of an area of the polar filament (PF). The spore has an electron-dense outer spore coat (exospore) overlying an inner thicker lucent region (endospore) followed by a membrane system surrounding the spore contents and polar filament coils (PF). The spore contents are composed of a complex of tightly packed arrays of membrane clusters and a centrally located sporoplasm, composed of scant cytoplasm containing a pair of abutted nuclei (diplokaryon), tightly packed ribosomes, and some endoplasmic reticulum. Surrounding this complex is a coiled polar filament (termed the polar tube (PT) when extruded) which becomes straight in the anterior part of the spore where it will exit when it is activated. The enlarged area of the PF coil cross sections illustrates the internal concentric rings and electron-dense particles (arrows) composing part of the internal structure of the PF. Images reprinted with permission from Cali A, Weiss LM, Takvorian PM (2002) *Brachiola algerae* spore membrane systems, their activity during

extrusion, and a new structural entity, the multilayered interlaced network, associated with the polar tube and the sporoplasm. J Eukaryot Microbiol 49 (2):164–174. doi:https://doi.org/10.1111/j.1550-7408.2002.tb00361.x (Cali et al. 2002)

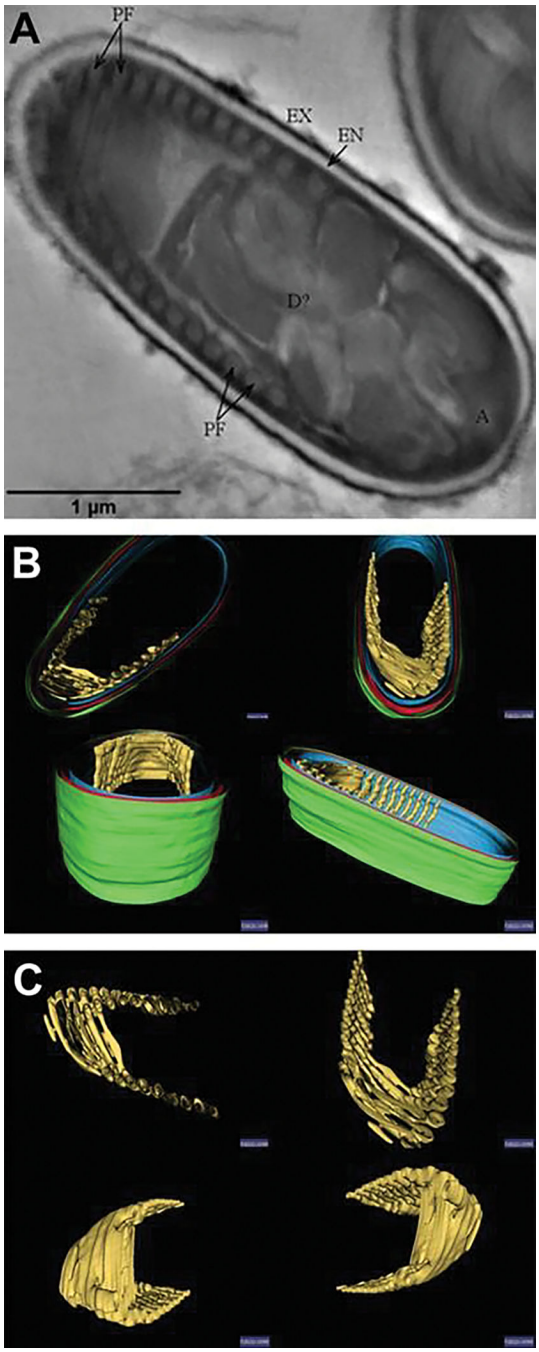

Fig. 8.3.

High-voltage (1.2million KV) transmission electron microscope images and three-dimensional models generated from the images of an *Anncaliia algerae* spore. (a) High-voltage transmission electron microscope (HVTEM) image of a 400-nm-thick section obtained with a 1.2 million accelerating voltage. One hundred and twenty one (121) images of the section were taken at 0–60^0 tilt angles at two degree increments from the four aspects for a total of 120 tilt images plus the original zero tilt position. The images were then aligned, “Z” stack, and a volume of the images was produced. Slice number 52 of the

volume is of a nonactivated *Anncaliia algerae* spore. The exospore (EX), endospore (EN), diplokaryion (D), anchoring disk (A), and polar filament (PF) are all visible. (b) HVTEM three-dimensional model of the spore generated from the 121 tilt series image volume segmented with Amira© software. The exospore (EX) is green, endospore (EN) is red, the spore wall inner membranes are blue, and the polar filament is gold in this rendering. The spore models are tilted to enable different viewing angles of the PF inside the spore. (c) HVTEM three-dimensional model of the segmented polar filament obtained from the volume in Fig. 8.3a. The model illustrates the uniform orientation of the PF. The models are tilted to enable different viewing angles of the PF. These various images were obtained by Dr. Peter M. Takvorian using equipment at the Resource for Visualization of Biological Complexity, NYS Department of Health Wadsworth Center, Empire State Plaza, P.O. Box 509, Albany, *NY* 12201, USA

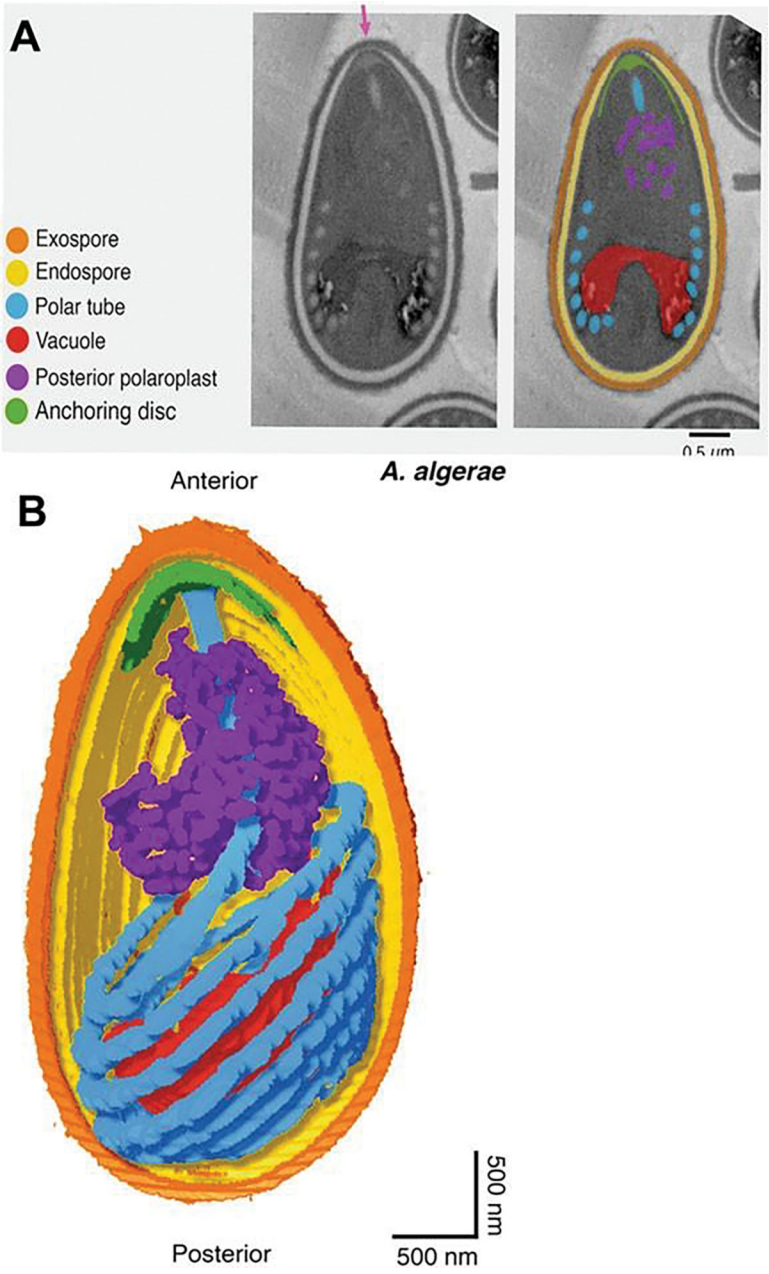

Fig. 8.4.

Serial block-face scanning electron microscopy (SBFSEM) imaging of intact *Anncaliia algerae* spores. (a) Serial block-face scanning electron microscopy imaging of intact *Anncaliia algerae* spores. Samples were serially sliced at 50 nm thickness (left), and images for a representative slice are shown. (b) Representative SBFSEM slice highlighting segmented organelles. Original micrograph is shown (left), as well as the same image with color overlays indicating segmented organelles (right): exospore (orange), endospore (yellow), PT (blue), vacuole (red), posterior polaroplast (purple), and anchoring disc (green). Magenta arrow indicates the thinnest part of the endospore layer where the anchoring disc is localized. (c) Representative 3D reconstruction of an *Anncaliia algerae* spore from SBFSEM

data. Each color represents an individual organelle, color code as in (b). Images reprinted with permission from Jaroenlak P, Cammer M, Davydov A, Sall J, Usmani M, Liang F-X, Ekiert D, Kroon G (2020a) 3-Dimensional organization and dynamics of the microsporidian polar tube invasion machinery. PLoS pathogens 16:e1008738. doi:https://doi.org/10.1371/journal.ppat.1008738 (Jaroenlak et al. 2020)

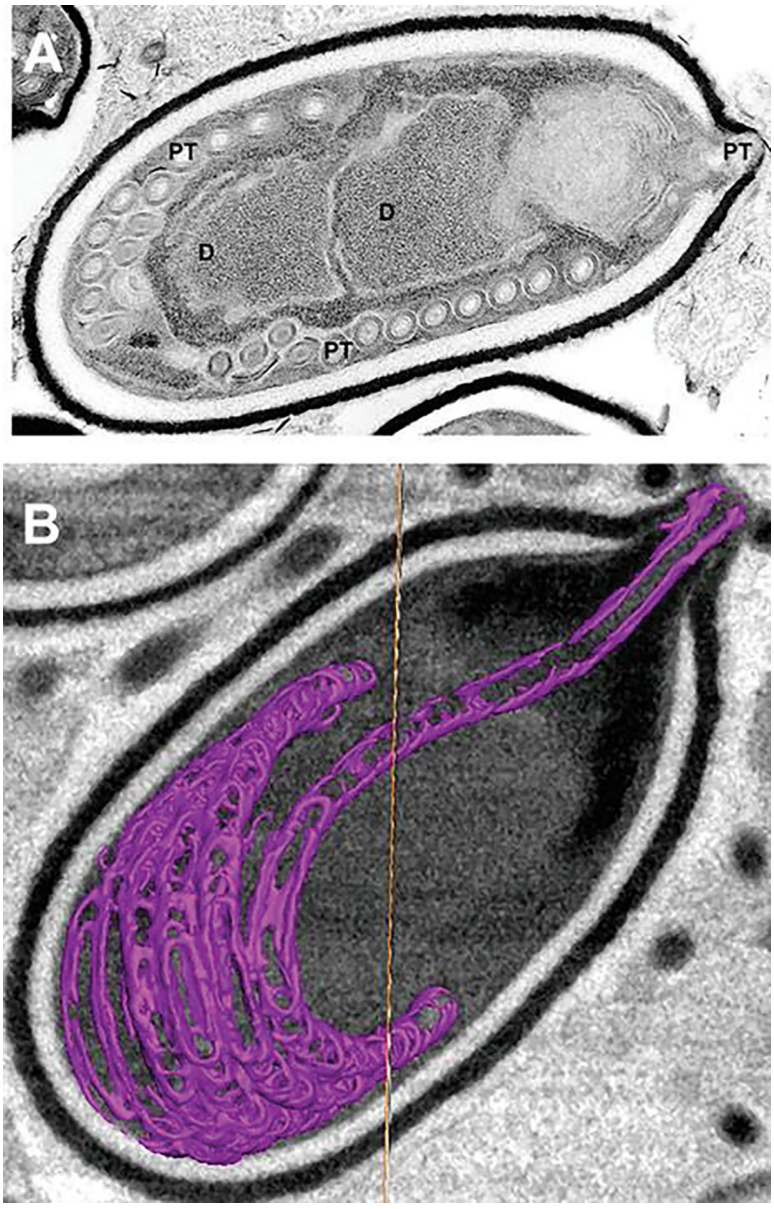

Fig. 8.5.

Transmission electron microscope (TEM) image and focused ion beam scanning electron microscope image of an activated *Anncaliia algerae* spore. (a) TEM image of an activated *Anncaliia algerae* spore starting the extrusion process. The internal organization of the spore undergoes massive membrane reorganization while the polar filament changes, becoming a hollow tube as it everts and starts exiting the spore through the anterior anchoring disk (A) and the opening of the spore wall. The PF has translocated, and the diplokaryon (D) is in the middle the spore and in a tandem relationship. (b) Focused ion beam scanning electron microscope (FIB-SEM) image from a tomogram generated from 15-nm-thick "Z" stack images of an activated *Anncaliia algerae* spore with an extruding polar filament. The polar filament was segmented with Amira© software to produce a 3-D rendering. The spore image has an overlay of the uncoiling polar filament (purple) exiting the anterior thin exospore

wall. The spore wall has erupted forming a collar through which the PT is exiting. The collar is composed of part of the anchoring disc, polaroplast, and exospore wall. These various images were obtained by Dr. Peter M. Takvorian with assistance from Dr. William J. Rice and Ashleigh Raczkowski using equipment at the Simons Electron Microscopy Center New York Structural Biology Center 89 Convent Avenue, NY, NY 10027

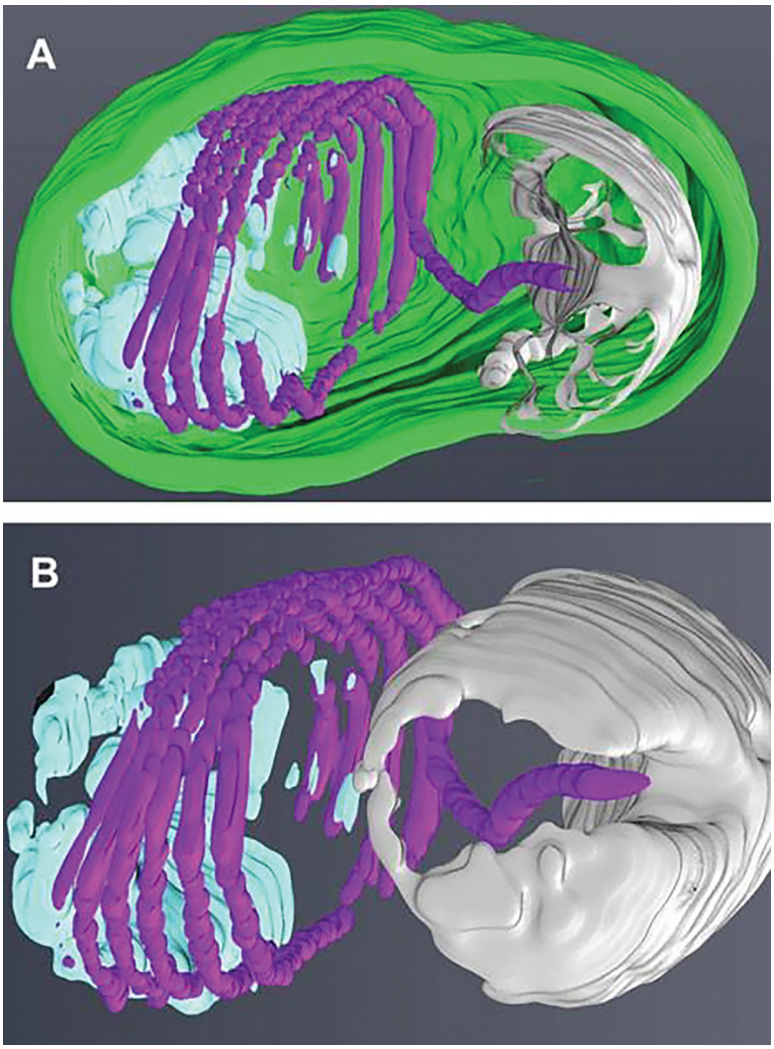

Fig. 8.6.

Three-dimensional models generated from “Z” stack images obtained from focused ion beam scanning electron microscopy (FIB-SEM). (a) A three-dimensional model generated from the 15-nm-thick “Z” stack image volume (see Fig. 8.5b) obtained with an FIB-SEM. The image stacks of the activated spore are aligned and then segmented with Amira© software. The segmented areas are the exospore (green), the anchoring disc-polaroplast complex (silver), the polar tube (purple), and the posterior vacuole and membranes (light blue). (b) A three-dimensional model of the segmented spore (see Fig. 8.5b) containing internal organelles, anchoring disc-polaroplast complex (silver), the polar tube (purple), and the posterior vacuole and membranes (light blue). The removal of the exospore wall and rotation of the model to show the anterior aspect of the PT and anchoring disc complex provides a view of the exiting PT passing through the complex as it uncoils and straightens. These various images were obtained by Dr. Peter M. Takvorian with assistance from Dr. William J. Rice and Ashleigh Raczkowski using equipment at the Simons Electron Microscopy Center New York Structural Biology Center 89 Convent Avenue, NY, NY 10027

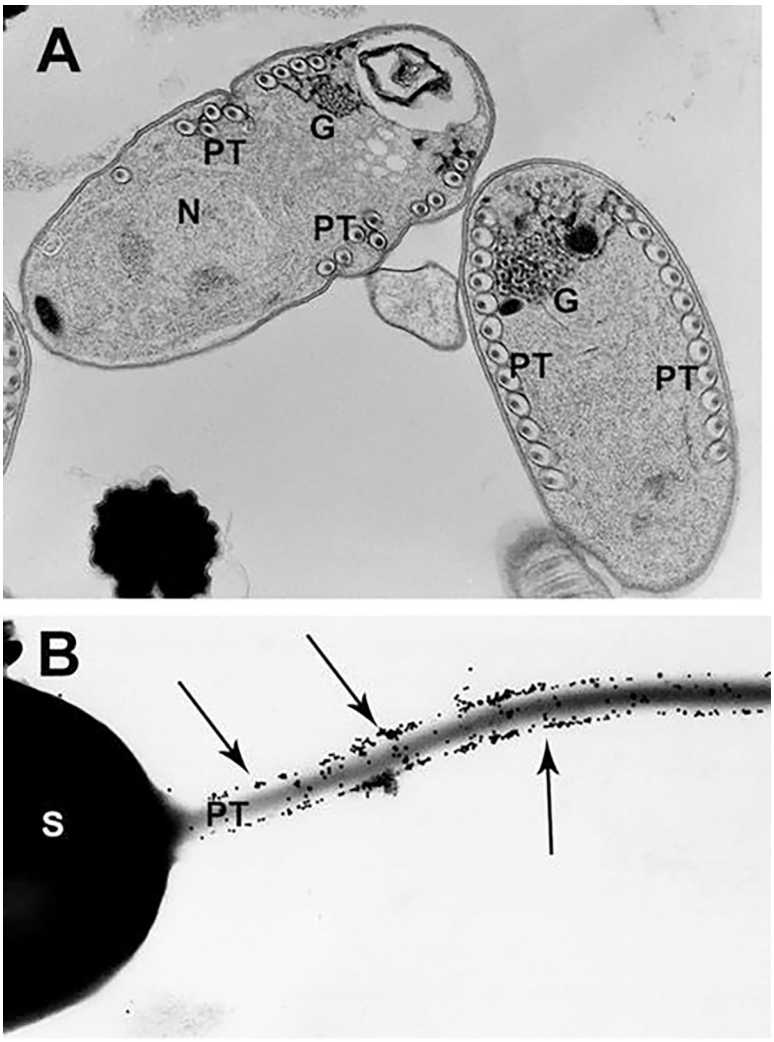

Fig. 8.7.

Transmission electron microscope (TEM) image of polar filament formation and post-transcriptional glycosylation of the filament involving the Golgi. (a) TEM image of *Glugea stephani* sporoblasts containing developing polar filaments (PF), enzyme histochemically labeled for Golgi. The electron-dense reaction product (RP) outlines each outer layer of the filament, and fenestrated clusters of RP are present on the Golgi complex-filament interface. During PF development, the polar tube proteins are posttranslationally modified by the Golgi. (b) TEM image of an *Anncaliia algerae* spore with extruding polar tube. The spore was immune-gold labeled to demonstrate the presence of Con A on the polar tube. Note the large numbers of 12-nm gold particle labeling the polar tube surface. Reprinted with permission from Xu Y, Takvorian PM, Cali A, Orr G, Weiss LM (2004) Glycosylation of the major polar tube protein of *Encephalitozoon hellem,* a microsporidian parasite that infects humans. Infection and immunity 72 (11):6341–6350. doi: https://doi.org/10.1128/IAI.72.11.6341-6350.2004 (Xu et al. 2004)

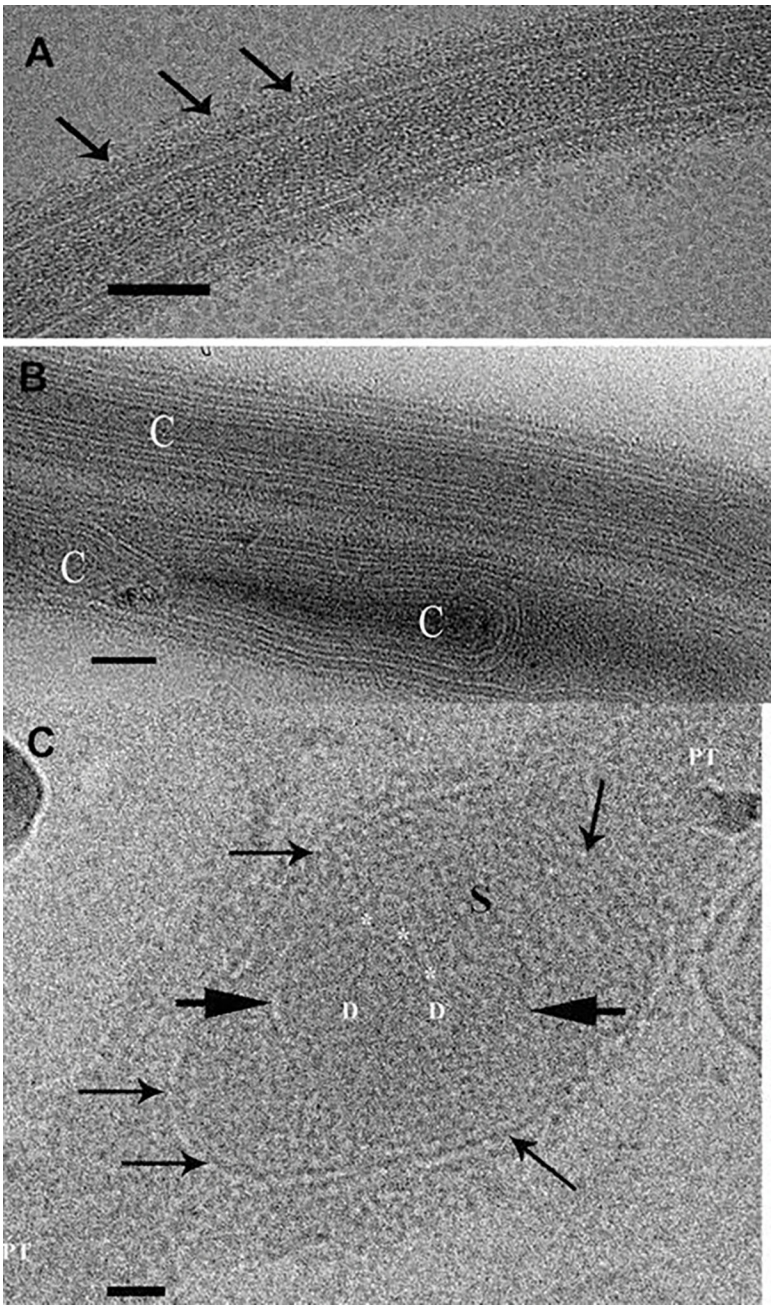

Fig. 8.8.

Transmission electron microscope images of *Anncaliia algerae* extruded polar tubes that are cryogenically preserved and imaged while frozen. (a) Cryo-TEM image of a cryogenically preserved extruded polar tube (PT). Multiple layers of varying densities are visible. The outermost surface edge is covered with the fine fibrils (arrows). Bar is 50 nm. (b) Cryo-TEM image of two polar tube (PT) segments that contain various forms of material. The upper tube has multiple layers of membrane-like material arranged parallel to the orientation of the tube and surrounding a narrow long cylinder (C). The lower PT contains membrane-like and tubular structures, some of which bend around cylinders (C). Bar is 50 nm. (c) Cryo-TEM

image of a polar tube (PT) that contains a membrane enclosed (arrows) sporoplasm (S) inside the tube. The oval- or sperm head-shaped sporoplasm has greatly distended a portion of the tube. The sporoplasm contains medium-dense material, and a membrane (short arrows) encloses two nuclei in a diplokaryon (D) arrangement. The membrane enclosed nuclear region has an indentation, and three or four small circular structures are abutted to it (*). Bar is 50 nm. Images reprinted with permission from Takvorian PM, Han B, Cali A, Rice WJ, Gunther L, Macaluso F, Weiss LM (2020) An Ultrastructural Study of the Extruded Polar Tube of *Anncaliia algerae* (Microsporidia). J Eukaryot Microbiol 67 (1): 28–44. doi:https://doi.org/10.1111/jeu.12751 (Takvorian et al. 2020)

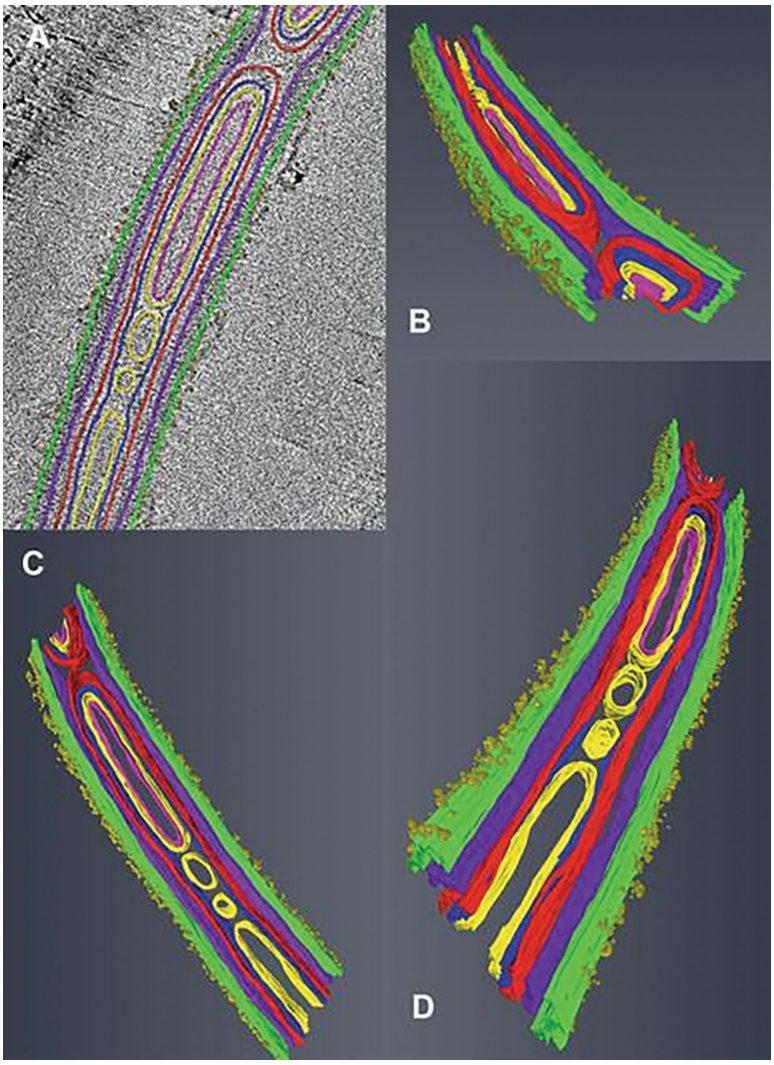

Fig. 8.9.

Tomograms and three-dimensional models generated from cryo-TEM "Z" stacks of aligned images. (a–d) Tomogram of a portion of polar tube (PT) containing membranes, cylinders, and its surface is covered with tufts of fibrillar material. The tomogram was segmented and 3D models were generated from it using Amira© software. The colors are assigned to different structures inside and on the surface of the polar tube. The fibril tufts are visible on the surface of the PT. The models are tilted at various angles to enable observation of different internal structures and their relationships. Images reprinted with permission from Takvorian PM, Han B, Cali A, Rice WJ, Gunther L, Macaluso F, Weiss LM (2020) An Ultrastructural Study of the Extruded Polar Tube of *Anncaliia algerae* (Microsporidia). J Eukaryot Microbiol 67 (1):28–44. doi:https://doi.org/10.1111/jeu.12751 (Takvorian et al. 2020)

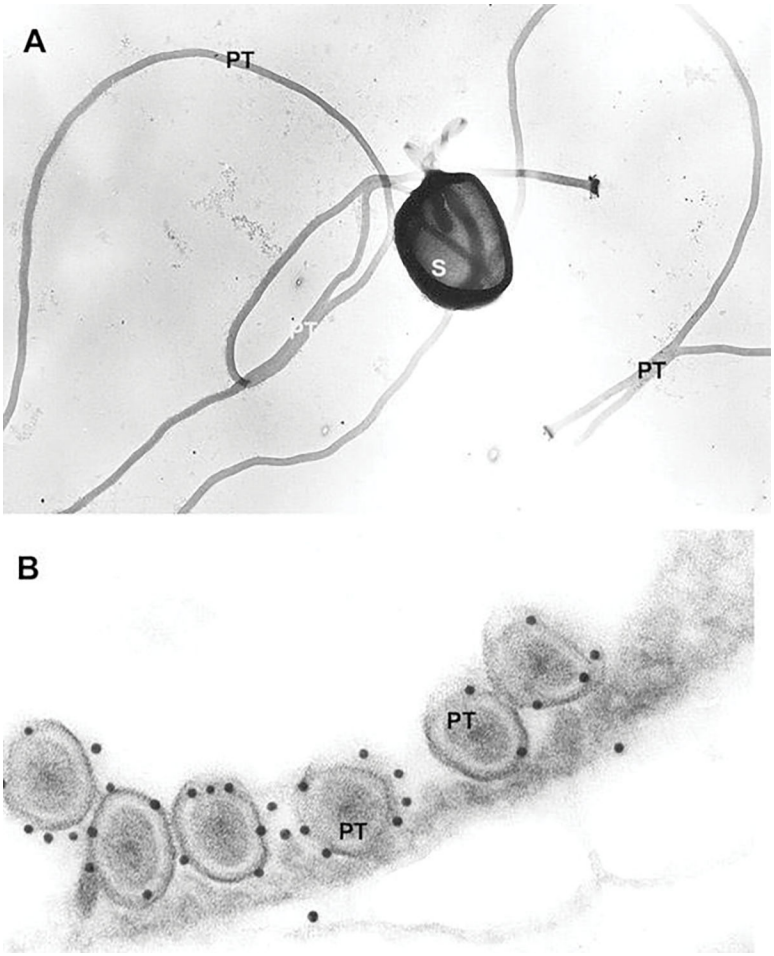

Fig. 8.10.

Transmission electron microscope images of a mechanically disrupted spore and polar tubes used during production of polar tube protein antibodies. (a) TEM image of *Glugea americanus* (*Spraguea americana*) spores mechanically disrupted with glass beads, washed in 1% SDS and 9 M urea, and negatively stained with uranyl acetate. The spore is broken open, part of the PT is still inside it, and several intact PTs are present. (b) TEM image of *Glugea americanus* (*Spraguea americana*) polar filament immunogold labeled for polar tube protein 1 (PTP-1). A cross section of six PF coils is visible and 12-nm gold secondary labels the primary antibody raised against PTP-1. Most of the gold is attached to the outer PT layer. Images reprinted with permission from Keohane EM, Orr GA, Takvorian PM, Cali A, Tanowitz HB, Wittner M, Weiss LM (1996) Identification of a microsporidian polar tube reactive antibody. J. Euk Microbiol. 43(1): 26–31. (Keohane et al. 1996)

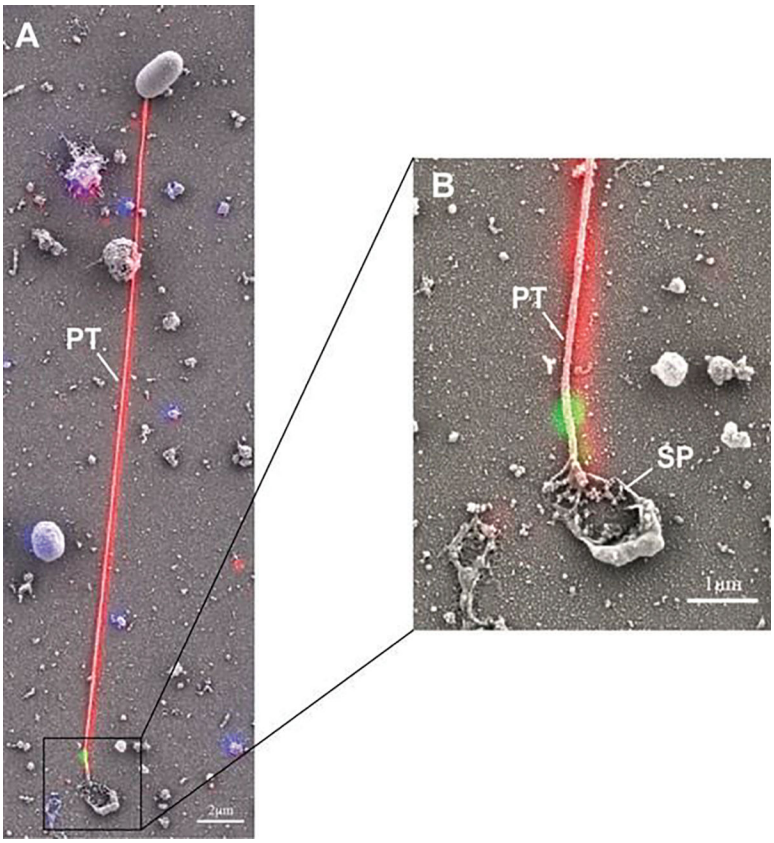

Fig. 8.11.

Correlative light and electron microscopy (CLEM) analysis of germination of *Encephalitozoon hellem. Encephalitozoon hellem*-infected tissue cultures were incubated with rabbit polyclonal to EhPTP1 (red) and murine monoclonal to EhPTP4 (green). The fluorescence image and SEM image of the same site were taken sequentially, and the fluorescence images with labeling of EhPTP4 and the polar tube were correlated to the SEM images which demonstrated the germination of a microsporidium at high resolution. Panel (a) shows an extruded polar tube with EhPTP4 staining at the end of the polar tube (PT). Panel (b) shows the enlarged section of panel (A), and the droplet of released sporoplasm (SP) was still attaching to the tip of polar tube. Reprinted with the permission from Han B, Polonais V, Sugi T, Yakubu R, Takvorian PM, Cali A, Maier K, Long M, Levy M, Tanowitz HB (2017a) The role of microsporidian polar tube protein 4 (PTP4) in host cell infection. PLoS pathogens 13 (4):e1006341 (Han et al. 2017)

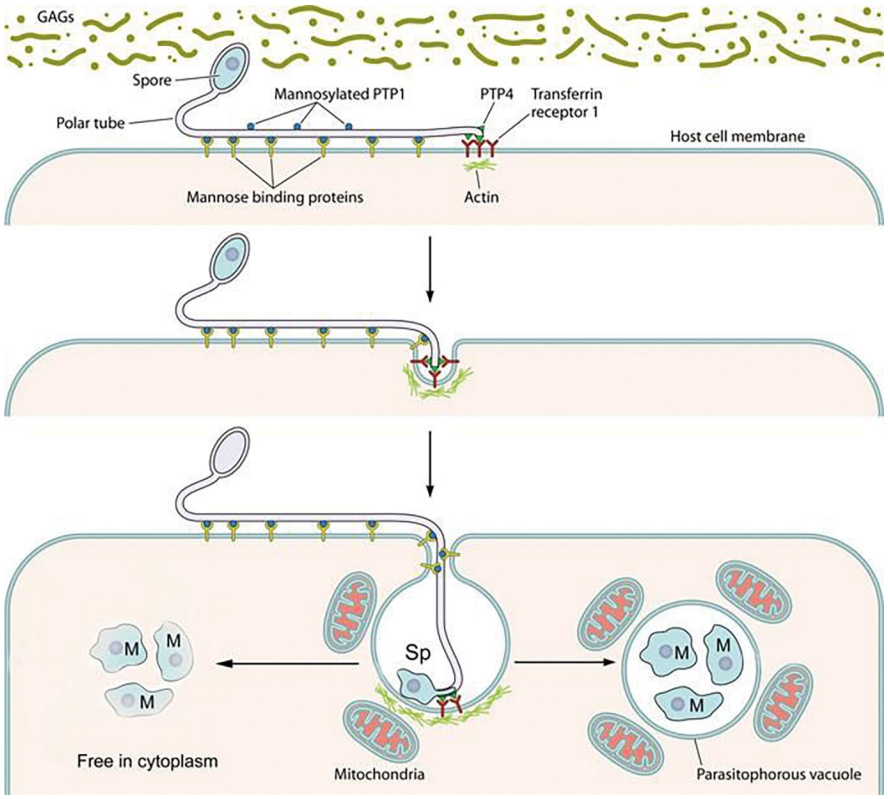

Fig. 8.12.

A model of polar tube adherence and invasion. This model is based primarily on data collected using *Encephalitozoon* spp. as a model for host cell invasion. The spore wall contains spore wall proteins (e.g., EnP1, NbSWP7, NbSWP9, NbSWP11, NbSWP12, and NbSWP16) that can interact and adhere to glycosaminoglycans (GAGs) and other substances in the mucin layer (green) of the gastrointestinal track or can interact with GAGs on the surface of host cells. These interactions are probably involved in germination. As the polar tube germinates, the polar tube adheres to the host surface by interactions of polar tube protein 1 (PTP1) with host cell surface mannose-binding proteins (MBP). This allows the polar tube to form an invasion synapse by pushing into the host cell membrane. In the formation of the invasion synapse, interactions of PTP1 (and possibly PTP4) with the host cell membrane result in the establishment of a protected microenvironment for the extruded microsporidian sporoplasm which excludes the external environment. Within the invasion synapse, epitopes of polar tube protein 4 (PTP4) that are exposed at the tip of polar tube interact with transferrin receptor 1 (TfR1), and possibly other host cell interacting proteins (HCIPs), at the host cell plasma membrane triggering signaling events. During the final steps of invasion, these various interactions lead to the formation of the invasion vacuole which can include clathrin-mediated endocytosis as well as the involvement of host cell actin. The sporoplasm (and meront) possess surface proteins, such as sporoplasm protein 1 (SSP1), which interact with various host cell surface proteins tethering the sporoplasm to the plasma membrane during invasion facilitating development of the invasion vacuole. At this early stage of infection, host mitochondria are already located around the invasion vacuole. For microsporidia that develop in the cytoplasm (arrow

on the left), such as *Nosema* spp. and *Anncaliia* spp., the organisms penetrate the invasion vacuole, and meronts can be seen undergoing development within the cytoplasm of the host cell. For microsporidia that develop in a parasitophorous vacuole (arrow on right), such as *Encephalitozoon* spp., the invasion vacuole completes its internalization of the sporoplasm; it becomes a meront and starts replicating. The meront surface interacts with the invasion vacuole membrane forming electron-dense membrane structures that allows meront SSP1 to interact with voltage-dependent anion selective channels (VDAC) located on the outer membrane of the mitochondria. The interaction of SSP1 and VDAC appears to play a crucial role in association of host cell mitochondria with the invasion vacuole facilitating energy acquisition from the host cell by replicating meronts. Adapted with permission from Han B, Pan G, Weiss LM (2021) Microsporidiosis in Humans. Clin Microbiol Rev.:e0001020. doi:https://doi.org/10.1128/CMR.00010-20 (Han et al. 2021)

Table 8.1

Polar tube proteins (PTPs)

	PTP1	PTP2	PTP3	PTP4	PTP5	PTP6
Encephalitozoon cuniculi	395 aa ECU06_0250	277 aa ECU06_0240	1256 aa ECU11_1440	276 aa ECU07_1090	251 aa ECU07_1080	238 aa ECU08_1710
Encephalitozoon intestinalis	371 aa Eint_060150	275 aa Eint_060140	1256 aa Eint_111330	279 aa Eint_071050	252 aa Eint_071040	234 aa Eint_081670 200 aa Eint_081680
Encephalitozoon hellem	453 aa 413 (EhATCC) EHEL_060170	272 aa EHEL_060160	1284 aa EHEL_111330	278 aa EHEL_071080	251 aa EHEL_071070	225 aa EHEL_081670
Encephalitozoon romalae	380 aa EROM_060160	274 aa EROM_060150	1254 aa EROM_111330	280 aa EROM_071050	251 aa EROM_071040	231 aa EROM_081700 198 aa EROM_081710
Antonospora locustae	355 aa ORF1050[a]	287 aa ORF1048[a] 568 aa (PTP2b) ORF1712[a] 599 aa (PTP2c) ORF1329[a]	Partial sequence	381 aa ORF969[a]	242 aa ORF968[a]	nd
Paranosema grylli	351 aa	287 aa	Partial sequence	381 aa	Partial sequence	nd
Enterocytozoon bieneusi	nd	283 aa EBI_26400	1219 aa EBI_22552	nd	nd	nd
Trachipleistophora hominis	nd	291 aa THOM_1756	1518 aa THOM_1479	Partial sequence THOM_1575	259 aa THOM_1161	153 aa THOM_2851
Nosema ceranae	456 aa NCER_101591	275 aa NCER_101590	1414 aa NCER_100083	208 aa NCER_100526	268 aa NCER_100527	185 aa NCER_100577
Nosema bombycis[b]	409 aa NBO_7g0016	277 aa AEK69415	1370 aa AEF33802	222 aa ACJZ01000169 (3927–4595)	271 aa ACJZ01002324 (213–1028)	247 aa NBO_1135G0001
Anncaliia algerae	407 aa KI0ABA33YN06FM1	3 partial sequences	1203 aa KI0APB23YG12FM1	254 aa KI0ANB26YM04FM1	240 aa KI0AGA10AA09FM1	nd
Vittaforma corneae	nd	293 aa VICG_01748	Partial sequence VICG_01948	254 aa VICG_01195	204 aa VICG_01807	nd
Vavraia culicis floridensis	nd	291 aa VCUG_00650	1864 aa VCUG_02017	372 aa VCUG_02471	356 aa VCUG_02366	nd
Edhazardia aedis	nd	307 aa EDEG_00335	1447 aa EDEG_03869 1284 aa EDEG_03429	465 aa EDEG_03857	252 aa EDEG_03856	nd
Nematocida parisii	nd	251 aa NEQG_02488	1177 aa NEQG_00122	nd	nd	nd

	PTP1	PTP2	PTP3	PTP4	PTP5	PTP6
Hamiltosporidium tvaerminnensis (Octosporea bayeri)	nd	nd	Partial sequence ACSZ01010190	Partial sequence ACSZ01005588	212 aa ACSZ01000826	nd

aa amino acids

nd not determined, probably because of high-sequence divergence or incomplete assembly of the genome. For PTP1, there are also some differences in the number of amino acids for different strains of *Encephalitozoon cuniculi* and *Encephalitozoon hellem* (Peuvel 2000)

Octosporea bayeri from Broad Institute (http://www.broadinstitute.org/annotation/genome/microsporidia_comparative/GenomesIndex.html)

[a] Antonospora locustae database (http://forest.mbl.edu/cgi-bin/site/antonospora01)

[b] *Nosema bombycis* (annotated sequences of *Nosema bombycis* and *Nosema antheraeae* are deposited in GenBank with the following accession numbers: ACJZ01000001-ACJZ01003558)